CHARACTERIZATION AND MODELING OF THORACO-ABDOMINAL RESPONSE TO BLAST WAVES

Volume 3. Lung Dynamics and Mechanical Properties Determination

Annual/Final Report

May 1985

Y. C. Fung, M. R. Yen, and Y. J. Zeng
University of California, San Diego

Contract No. DAMD17-82-C-2062

Supported by

U. S. Army Medical Research and Development Command
Fort Detrick, Frederick, Maryland 21701

The findings in this report are not to be construed as an official Department of the Army position unless so designated by other authorized documents.

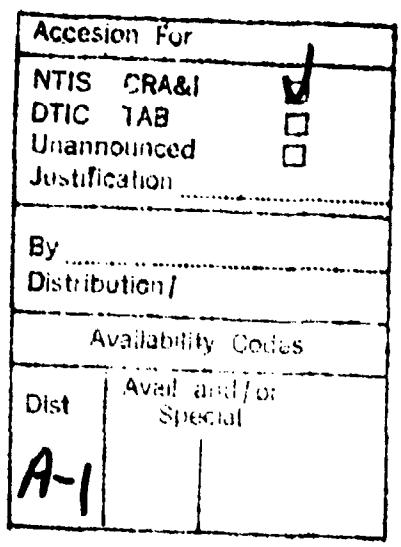

SECURITY CLASSIFICATION OF THIS PAGE

REPORT DOCUMENTATION PAGE

Form Approved OMB No. 0704-0188

1a. REPORT SECURITY CLASSIFICATION UNCLASSIFIED	1b. RESTRICTIVE MARKINGS
2a. SECURITY CLASSIFICATION AUTHORITY	3. DISTRIBUTION/AVAILABILITY OF REPORT Approved for public release; distribution unlimited
2b. DECLASSIFICATION/DOWNGRADING SCHEDULE	
4. PERFORMING ORGANIZATION REPORT NUMBER(S)	5. MONITORING ORGANIZATION REPORT NUMBER(S)
6a. NAME OF PERFORMING ORGANIZATION JAYCOR — 6b. OFFICE SYMBOL (If applicable)	7a. NAME OF MONITORING ORGANIZATION
6c. ADDRESS (City, State, and ZIP Code) 11011 Torreyana Road San Diego, California 92121	7b. ADDRESS (City, State, and ZIP Code)
8a. NAME OF FUNDING/SPONSORING ORGANIZATION U.S. Army Medical Research & Development Command — 8b. OFFICE SYMBOL (If applicable)	9. PROCUREMENT INSTRUMENT IDENTIFICATION NUMBER DAMD17-82-C-2062
8c. ADDRESS (City, State, and ZIP Code) Fort Detrick Frederick, Maryland 21701-5012	10. SOURCE OF FUNDING NUMBERS PROGRAM ELEMENT NO. 61102A — PROJECT NO. 3M1 61102BS10 — TASK NO. CG — WORK UNIT ACCESSION NO. 087

11. TITLE (Include Security Classification)
(U) Characterization and Modeling of Thoraco-Abdominal Response to Blast Waves
Volume 3. Lung Dynamics and Mechanical Properties Determination

12. PERSONAL AUTHOR(S)
Y. C. Fung, M. R. Yen, and Y. J. Zeng

13a. TYPE OF REPORT	13b. TIME COVERED	14. DATE OF REPORT (Year, Month, Day)	15. PAGE COUNT
Annual/Final	FROM 2/15/82 TO 5/31/85	1985 May	67

16. SUPPLEMENTARY NOTATION
Annual covers time period of 15 February 1984 - 31 May 1985.
Annual/Final published in 8 volumes

17. COSATI CODES			18. SUBJECT TERMS (Continue on reverse if necessary and identify by block number)
FIELD	GROUP	SUB-GROUP	
06	21		
06	17		

19. ABSTRACT (Continue on reverse if necessary and identify by block number)

20. DISTRIBUTION/AVAILABILITY OF ABSTRACT	21. ABSTRACT SECURITY CLASSIFICATION
☐ UNCLASSIFIED/UNLIMITED ☒ SAME AS RPT. ☐ DTIC USERS	Unclassified
22a. NAME OF RESPONSIBLE INDIVIDUAL Mary Frances Bostian	22b. TELEPHONE (Include Area Code) 301-663-7325 — 22c. OFFICE SYMBOL SGRD-RMI-S

DD Form 1473, JUN 86 — Previous editions are obsolete. — SECURITY CLASSIFICATION OF THIS PAGE

FOREWORD

This Annual/Final Report has eight volumes. The titles are as follows:

1. Project Summary
2. Blast Load Definition on a Torso Model
3. Lung Dynamics and Mechanical Properties Determination
4. Biomechanical Model of Thorax Response to Blast Loading
5. Experimental Investigation of Lung Injury Mechanism
6. Biomechanical Model of Lung Injury Mechanisms
7. Gastrointestinal Response to Blast
8. Effect of Clothing on Thoracic Response

CONTENTS

ILLUSTRATIONS

TABLES

1. INTRODUCTION

OVERVIEW OF EXPERIMENTAL APPROACH AND EQUIPMENT

Four distinct experiments are performed to determine the mechanical properties of lung tissue:

1. Measurement of the incremental bulk modulus, K. The equipment imposes incremental changes to the lung volume and measures the corresponding transpulmonary pressure. From the pressure-volume curves the bulk modulus is computed. Figure 1-1 shows a photograph of this equipment. Details of analysis and results are presented in Section 2.1.

2. Measurement of the incremental Young's modulus, E. Two types of measurements are done:

   a. A known vertical deflection is applied on the pleural surface and the corresponding vertical load is measured.

   b. A circular flexible polyethylene membrane of various diameters (7 mm to 16 mm, depending on the size of the lung) is cemented to a flat portion of the pleura, and a vertical deflection is applied on the center of the membrane. The corresponding vertical load is measured. Figure 1-2 shows a photograph of this equipment. Performance has been thoroughly tested and is satisfactory. Details of the experiments and their results are presented in Section 2.2.

3. Measurement of material constants for human lungs in large deformation. This consists of two parts:

   a. The TRIAX testing machine, designed and constructed in our laboratory earlier, was used to measure the tissue components of the human lung stress-strain relationship. Figure 1-3 shows the equipment. New effort was made to adapt a new computer in the laboratory, PDP 1103, to perform on-line experiments and analysis. This has been accomplished. Results are contained in Section 2.3.

   b. Pressure-volume curves of air-filled human lungs are measured. This work is done in Dr. Sobin's laboratory in Los Angeles where fresh specimens can be obtained and tested as soon as they arrive in the laboratory.

Cont'd

4. Measurement of Wave Propagation in the Lung. For convenience of detailed examination, excised lungs are used. A small shock tube is used to impose impact loading on the lung. Pressure transducers are used to sense the shock and the stress waves. The speed of wave propagation is determined from the first arrival time of the pressure wave front and known distance between sensors. Figure 1-4 shows one of the two shock tubes designed and constructed. Figure 1-5 shows the test setup for the lung. Results are presented in Section 3.

Keywords: wounds and injuries; blast waves; blast loads; stress (physiology)

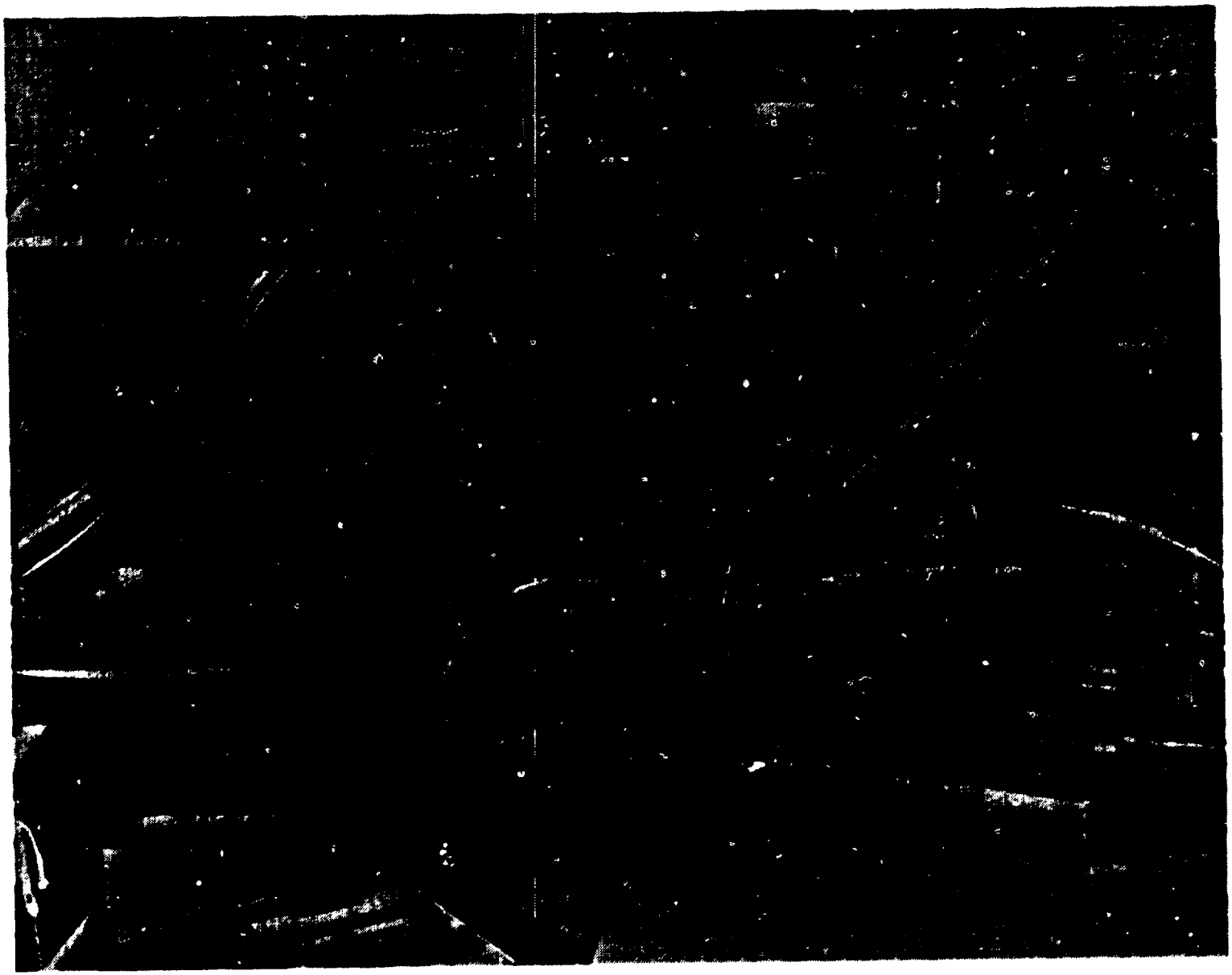

Figure 1-1. Equipment for measuring incremental bulk modulus of lung parenchyma by imposing increments of volume of the lung and measuring the corresponding transpulmonary pressures

Figure 1-2. Equipment for measuring incremental Young's modulus of lung parenchyma by indentation and by flexible disk

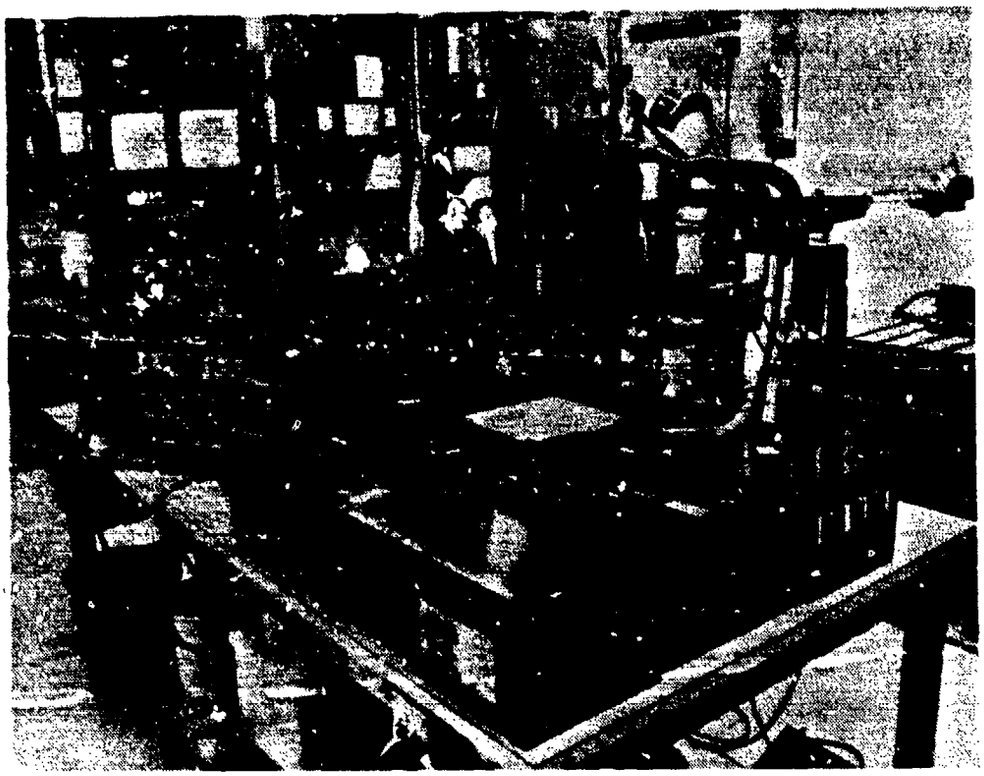

Figure 1-3(a). The Triax testing machine for determining the stress-strain relationship of lung in large deformation

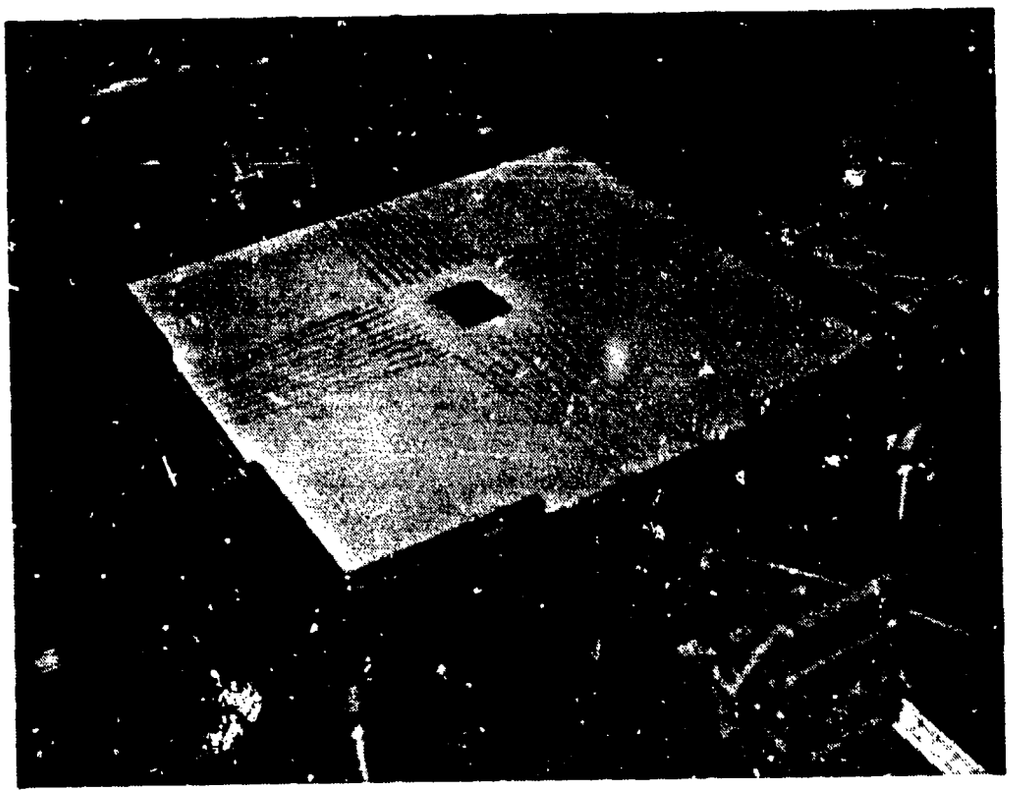

Figure 1-3(b). Test specimen, strain measuring target, loading strings, force transducers and thermally controlled bath

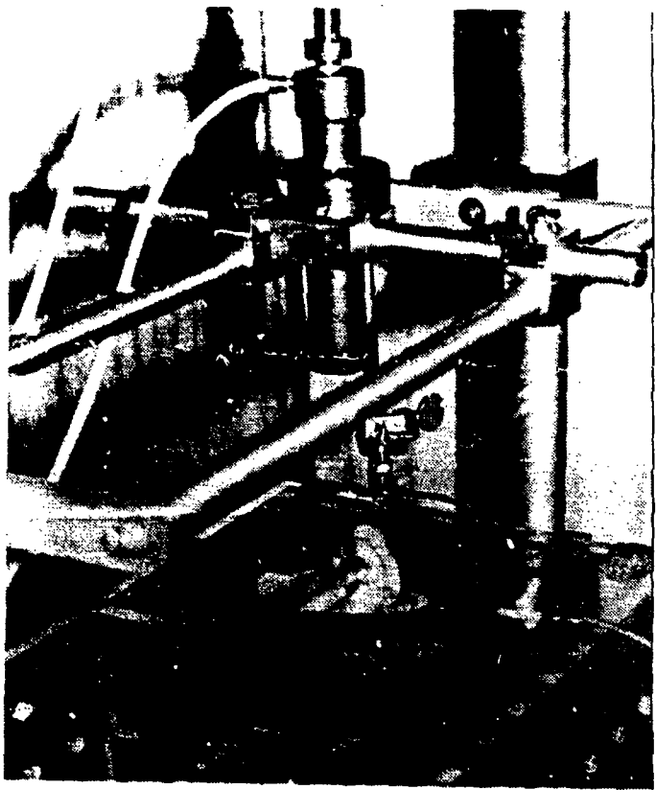

Figure 1-4. Shock tube for imposing impact loading on the surface of the lung

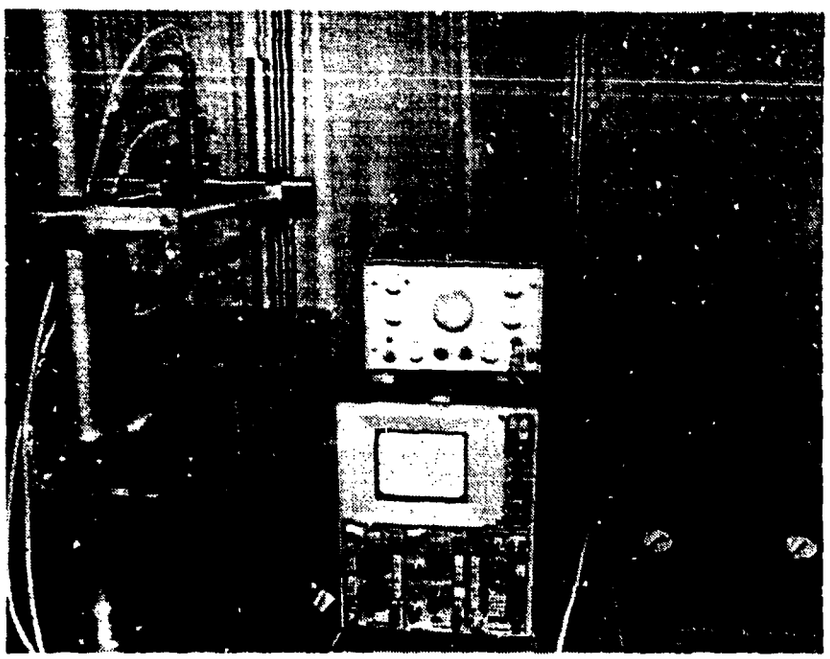

Figure 1-5. The test equipment for measuring elastic waves in the lung

2. LUNG PARENCHYMA MECHANICAL PROPERTIES

2.1 INCREMENTAL BULK MODULI OF ELASTICITY OF THE LUNG

2.1.1. Definitions

In the lung, the stress acting on any cross section consists of two parts: the stress due to stretching of the lung tissue (σ_{tissue}), and the alveolar gas pressure (P_A). We write

$$\text{stress} = \sigma_{tissue} - \alpha p_A \quad , \tag{2.1-1}$$

where α is the fraction of the cross section that is exposed to the alveolar gas, $1-\alpha$ is the fraction occupied by the interalveolar septa. See Figure 2.1-1. On the boundary of the lung is the visceral pleura. One side of the pleura is exposed to the pleural pressure p_{PL}. The other side is exposed to the stress given by Eq. (2.1-1). The tension in the pleura can be expressed in terms of the principal stress resultants, T_1 and T_2 per unit length. Let the principal curvatures of the pleura be $1/R_1$, and $1/R_2$, respectively. Then the condition of equilibrium of the pleura is (Fig. 2.1-2):

$$\sigma_{tissue} - \alpha p_A + p_{PL} = \frac{T_1}{R_1} + \frac{T_2}{R_2} \quad . \tag{2.1-2}$$

Due to the weight of the lung, or motion of the chest, the stress in the lung is nonuniform and the equilibrium of the lung requires the tension in the pleura. But if the right-hand side of Eq. (2.1-2) vanishes, then

$$\sigma_{tissue} = \alpha p_A - p_{PL} \quad . \tag{2.1-3}$$

σ_{tissue} is a function of the strains in the lung. If homogeneous strain is assumed, then σ_{tissue} is a function of the lung volume; so are p_A and p_{PL}. The volumetric strain of the lung being the ratio of change of volume of the lung to the lung volume, $\Delta V_{lung}/V_{lung}$, the incremental volumetric (or bulk) modulus of elasticity of the lung tissue is defined as

$$K_{tissue} = V_{lung} \frac{d\sigma_{tissue}}{dV_{lung}} = V_{lung} \frac{d(\alpha p_A - p_{PL})}{dV_{lung}} \quad . \tag{2.1-4a}$$

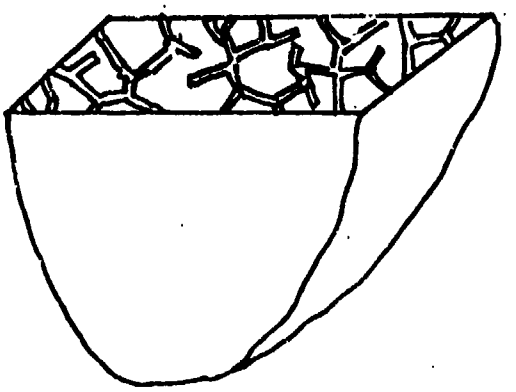

Figure 2.1-1. Concept of macroscopic stress defined over a small cross section of the lung tissue enclosing a number of alveoli and ducts.

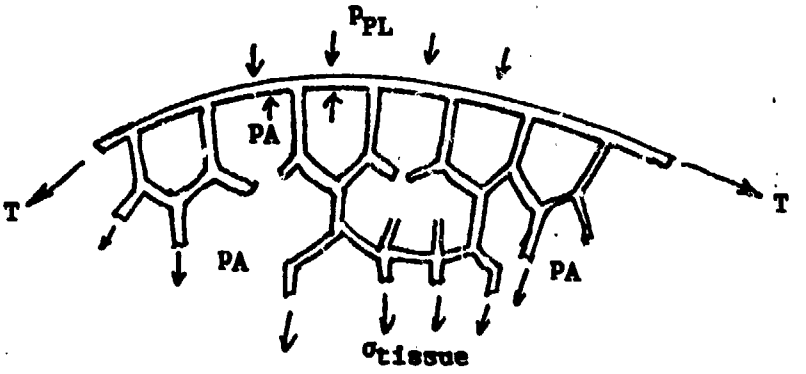

Figure 2.1-2. An enlargement of a small element of pleura, showing exposure to pleural pressure (p_{PL}) on one side, and to alveolar gas (p_A) and interalveolar septa on the other. The tension in the pleura multiplied by the curvature of the pleura is equivalent to a lateral load, and contributes to the balance of forces in the direction normal to the pleural surface, resulting in the terms on the right-hand side of Eq. (2.1-2).

This is the modulus relevant to the study of breathing, and is normally measured by experiments in which either p_A or p_{PL} is varied, with the airway open.

In the study of response of the lung to shock waves, it is relevant to consider the case in which the glottis is closed. The shock process is so fast that the bulk movement of gas through the glottis is negligible in the first few moments. In the closed glottis experiments, we may define the following incremental volumetric moduli of elasticity:

$$K_{lung} = V_{lung} \frac{dp_A}{dV_{lung}} , \qquad (2.1\text{-}4b)$$

$$K_{PL} = - V_{lung} \frac{dp_{PL}}{dV_{lung}} . \qquad (2.1\text{-}4c)$$

We shall call K_{PL} the "chest bulk modulus." K_{PL} is of interest to the calculation of the chest volume in response to shock waves enveloping the chest. K_{tissue} is of interest to the assessment of the stresses in the lung tissue, and hence of its strength and damage.

From Eqs. (2.1-4a), (2.1-4b), and (2.1-4c) we obtain

$$\alpha K_{lung} + K_{PL} = K_{tissue} . \qquad (2.1\text{-}5)$$

2.1.2. Open Airway Experiments

An experiment was designed to impose increments of volume to the lung while allowing air transfer between the inside and outside of the lung. An excised lung is suspended inside a lucite box. Air volume in the lung is varied by a pump connected to the trachea cannula while airway pressure (p_A) is measured and external pressure (p_{PL}) is held atmospheric. The bulk modulus is computed from pressure-volume curves obtained in this fashion. Figure 2.1-3 shows a typical p-v curve.

Results are shown in Table 2.1-1. It is seen that the magnitude of the bulk modulus of the lung tissue of the rabbit is of the order of 3 or 4 times the transpulmonary pressure. Lai-Fook (1979) has shown that K_{tissue} of dog lung is of a similar magnitude. Table 2.1-2 shows the results for cats and humans.

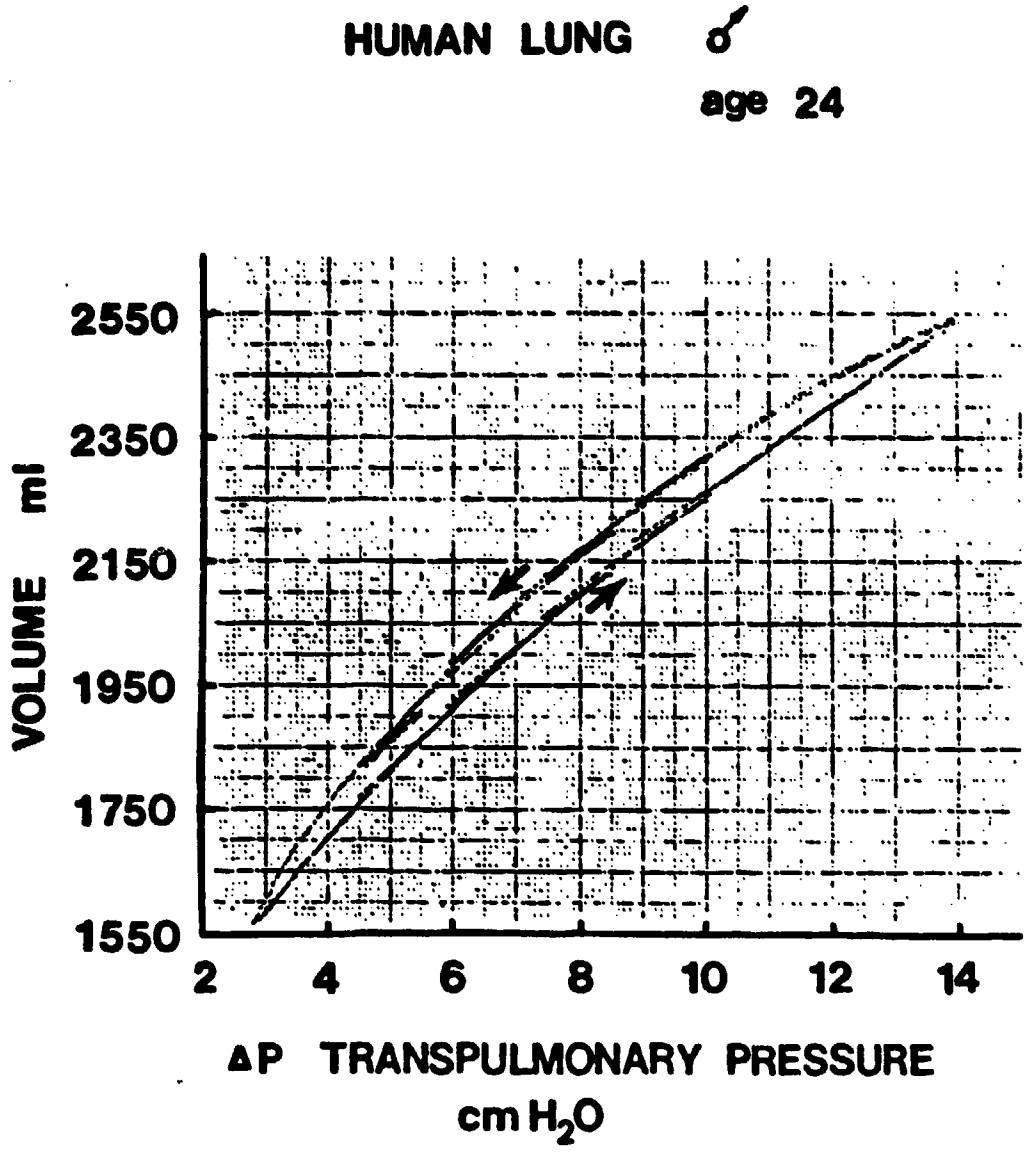

Figure 2.1-3. Pressure-volume curves of air-filled human lung

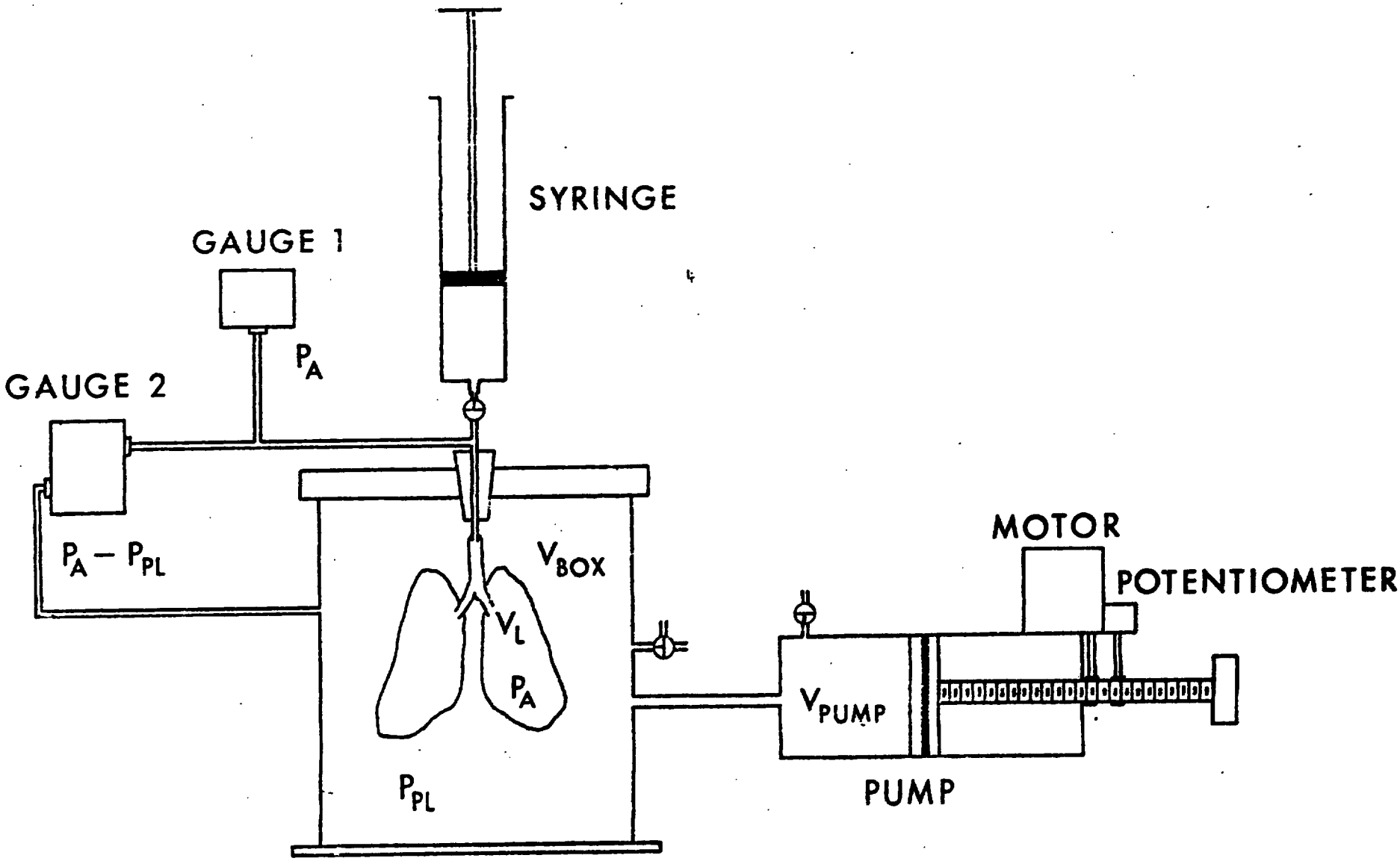

Figure 2.1-4. Schematic drawing of the bulk modulus measuring equipment.

Table 2.1-1. The Bulk Modulus of the Lung Tissue (K_{tissue}) of the Rabbit Determined by Open Airway Experiments

	Transpulmonary Pressure $P_A - P_{PL}$ (cm H_2O)	n	K_{tissue} (cm H_2O)	
			Mean	± S.D.
Inflation	4	4	13.60	2.42
Deflation	4	4	12.26	0.65
Inflation	6	4	21.32	1.62
Deflation	6	4	15.07	0.46
Inflation	8	4	30.69	2.21
Deflation	8	4	28.35	1.31
Inflation	10	4	36.87	3.70
Deflation	10	4	40.99	2.15

Table 2.1-2. The Bulk Modulus of Lung Tissue

a. Cats' Lung Tissue

	Transpulmonary Pressure $P_A - P_{PL}$ (cm H_2O)	n	K_{tissue} (cm H_2O) Mean	S. D.
Inflation	4	3	15.62	2.45
Deflation	4	3	12.19	2.07
Inflation	6	3	32.27	3.83
Deflation	6	3	26.16	5.15
Inflation	8	3	49.59	7.38
Deflation	8	3	46.03	11.52
Inflation	10	3	64.47	12.13
Deflation	10	3	61.89	15.30

b. Human Lung Tissue

	Transpulmonary Pressure $P_A - P_{PL}$ (cm H_2O)	K_{tissue} (cm H_2O)
Inflation	5	18.10
Deflation	5	21.94
Inflation	6.5	21.77
Deflation	6.5	25.40
Inflation	8	26.19
Deflation	8	28.73
Inflation	9.5	29.57
Deflation	9.5	29.80

2.1.3. Closed Airway Experiments

Equipment and Method

The equipment sketched in Figure 2.1-3 was used. The volume of air in the box and external to the lung can be varied by a Harvard infusion-withdrawal pump.

The calculation needs the volume of the lung tissue. This was obtained by measuring the volume of a completely atelectatic lung. The lungs of the animal under anesthesia were ventilated with 100% pure oxygen for one hour and then the trachea was clamped off. The gas in the lungs was then quickly absorbed by the circulating blood and the lungs collapsed completely. After excision, the volume of the tissue was determined by immersing it in water and measuring the rise of water surface in a tube.

The lung was then hung in the airtight lucite box. A known volume of air was then injected using a syringe so as to open all airspaces, creating an airway pressure of about 20-25 cm H_2O while the pleural pressure was atmospheric. For each experiment, a known volume of air was added or withdrawn from the lung using a syringe to obtain a desired initial p_A while $p_{PL} = 0$. The airway valve was then closed. Further change of lung volume was imposed by the infusion-withdrawal pump. In each change of volume the corresponding transpulmonary pressure (tracheal pressure minus pleural pressure) and the airway pressure were measured simultaneously using the Validine pressure transducers. During the experiment, the airway pressure was recorded using a strip-chart recorder, and the pump volume was plotted against pulmonary pressure using an x-y recorder. An x-y recorder was used also to plot change of p_A versus change of $p_A - p_{PL}$. These values are used to compute the bulk moduli.

Analysis

The volume of the lung is the sum of the volume of gas in the lung ($V_{alv.gas}$) and the volume of the lung tissue (V_{tissue}). Hence

$$V_{lung} = V_{alv.gas} + V_{tissue} \quad .$$

Since the airway and the external chamber are both closed, we have, by gas law,

$$p_A \cdot V_{alv.gas} = M_A RT \quad . \qquad (2.1\text{-}6)$$

Hence, when p_{PL}, p_A, and $V_{alv.gas}$ are changed by Δp_{PL}, Δp_A, and $\Delta V_{alv.gas}$, we have

$$(p_A + \Delta p_A)(V_{alv.gas} + \Delta V_{alv.gas}) = M_A RT \quad ;$$

$$\Delta V_{lung} = \frac{M_A RT}{p_A + \Delta p_A} - V_{alv.gas}$$

$$= - \frac{\Delta p_A}{p_A + \Delta p_A} V_{alv.gas} \quad . \tag{2.1-7}$$

Substituting this into the definition of chest bulk modulus Eq. (2.1-4c), we obtain

$$K_{PL} = \frac{V_{lung}}{V_{alv.gas}} \frac{\Delta p_{PL}}{\Delta p_A} (p_A + \Delta p_A) \quad . \tag{2.1-8}$$

On the other hand, for lungs with closed airways, Eq. (2.1-6) implies

$$\frac{dp_A}{p_A} + \frac{dV_{alv.gas}}{V_{alv.gas}} = 0 \quad .$$

Hence on substituting into Eq. (2.1-4b), we obtain the bulk modulus of the lung in the case of closed glottis:

$$K_{lung} = - \frac{V_{lung}}{V_{alv.gas}} p_A \quad . \tag{2.1-9}$$

Then by Eq. (2.1-5),

$$K_{tissue} = \frac{V_{lung}}{V_{alv.gas}} \frac{\Delta p_{PL}}{\Delta p_A} (p_A + \Delta p_A) - \alpha p_A \quad . \tag{2.1-10}$$

Since α is an unknown anatomical parameter, we compute a $\bar{K}$ for closed airway defined by Eq. (2.1-10) with $\alpha = 1$:

$$\bar{K} = \frac{V_{lung}}{V_{alv.gas}} \frac{\Delta p_{PL}}{\Delta p_A} (p_A + \Delta p_A) - p_A \quad , \tag{2.1-11}$$

then

$$K_{tissue} = \bar{K} + (1 - \alpha) p_A \frac{V_{lung}}{V_{alv.gas}} \quad . \tag{2.1-12}$$

Results

Table 2.1-3 shows a set of typical results on an animal. It shows the similarity, with opposite signs, of the values of the chest bulk modulus and lung gas modulus when the airway is closed. The sum yields the bulk modulus of the lung tissue.

Table 2.1-4 summarizes the experimental results of the rabbit lung.

Discussion

The chest bulk modulus, K_{PL}, for lung experiments with glottis closed, is seen to be much larger than the bulk modulus of the lung tissue, K_{tissue}. K_{PL} is nearly equal to the bulk modulus of the air in the lung.

The K_{tissue} values obtained from closed airway experiments are seen to be different from those obtained from open airway experiments. The reason for this discrepancy is not clear. The major difference to the lung tissue in these two experiments is that when the airway is closed very large changes in both pleural and airway pressures are required to obtain a small change in the transmural pressure, $p_A - p_{PL}$, whereas in the open airway experiments p_{PL} is kept constant and Δp_A is exactly equal to $\Delta(p_A - p_{PL})$. Lung inflation is, as is seen from Eqs. (2.1-2) and (2.1-3), essentially a function of the transmural pressure $p_A - p_{PL}$, but blood vessels respond to (blood pressure - p_A) in the capillaries and to (blood pressure - p_{PL}) in the large vessels. Hence the blood vessels must be deformed to a very different degree in these two cases. The pleura contains bronchial and lymph vessels and must recognize the difference similarly. Further, we have lumped the airway (the part in the test box) with the lung in the data analysis, and treated the stress in the lung as homogeneous. Whether these factors explain the difference in K_{tissue} from open and closed airway experiments or not remains to be investigated.

2.2 INCREMENTAL YOUNG'S MODULUS OF ELASTICITY

Once the bulk modulus K of the lung tissue is determined, it is possible to obtain results for the shear modulus G, Young's modulus E, and Poisson's ratio ν through the indentation test.

Table 2.1-3. Closed Airway Experimental Results and Calculation of the Chest Bulk Modulus of Rabbit

V_A (ml)	V_{lung} (ml)	$p_A - p_{PL}$ (cm H_2O)	$\Delta(p_A - p_{PL})$ (cm H_2O)	p_A (cm H_2O)	Δp_A (cm H_2O)	p_{PL} (cm H_2O)	Δp_{PL} (cm H_2O)	K_{PL} (cm H_2O)	K_{lung} (cm H_2O)	K_{tissue} (cm H_2O)
71	87	10.71	-0.77	1045.3	8.93	1034.6	9.7	1403	-1281	122
69	85	8.94	-0.89	1043.0	11.03	1034.0	11.92	1403	-1285	118
67	83	7.41	-0.62	1041.3	10.84	1034.5	11.46	1378	-1290	88
65	81	6.41	-0.41	1040.4	10.60	1029.8	11.01	1360	-1296	64
63	79	5.26	-0.24	1039.1	10.81	1028.3	11.05	1346	-1303	43

Table 2.1-4. Bulk Moduli of Rabbit Lung Obtained from Closed Airway Experiments

	Transpulmonary Pressure $P_A - P_{PL}$ (cm H_2O)	n	K_{PL} (cm H_2O)		K_{lung} (cm H_2O)		K_{tissue} (cm H_2O)	
			Mean	S.D.	Mean	S.D.	Mean	S.D.
	5.2	4	1316	37.4	-1298	31.8	18	9.0
I	5.7	4	1319	39.1	-1293	31.9	26	8.0
N								
F	6.1	4	1324	41.6	-1288	33.1	36	10.0
L								
A	6.7	4	1333	42.7	-1282	32.6	51	10.7
T								
I	7.4	4	1350	38.1	-1279	32.5	71	9.8
O								
N	8.4	3	1366	36.0	-1276	39.2	91	5.5
	10.8	3	1400	26.7	-1272	35.0	128	8.9
	4.4	3	1343	41.4	-1319	28.9	23	16.0
D	5.3	3	1345	30.5	-1308	26.4	37	7.1
E								
F	6.4	3	1359	25.0	-1300	26.2	59	4.2
L								
A	7.4	3	1371	25.2	-1293	26.1	78	8.5
T								
I	8.9	3	1391	21.4	-1287	25.1	104	14.0
O								
N	10.7	3	1406	10.3	-1282	24.0	124	14.1
	11.2	3	1410	9.9	-1281	24.0	129	16.8

2.2.1. Apparatus

A photograph of the equipment used in this test is shown in Figure 2.2-1. It consists of a Mitutoyo deflection apparatus (accurate to a 0.005 mm deflection), Statham pressure transducer (Model UC3), a Hewlett Packard 311A transducer amplifier-indicator, a Hewlett Packard 7100 BM strip chart recorder, and a manometer, which was used to inflate the lung to various pressures. The pressure transducer had a highly sensitive (3.175 mm diameter) probe which was mechanically attached to the deflection apparatus. This setup made it possible to measure the resistive load of the lung tissue resulting from an applied (known) deflection. The signal from the pressure transducer was then amplified and transmitted to the strip chart recorder where the load could be accurately measured.

The pressure transducer was calibrated with a dual-arm balance; a 50 gm weight was placed on one end while the probe was placed on the other end. The deflection apparatus was utilized to move the probe up or down until the balance arm was completely leveled, which implied that the probe was sensing the full 50 gm. The range of the strip chart recorder was then reduced since only small deformations were involved. Under such conditions the stress-strain relationship of the lung is considered to be linear.

2.2.2. Experimental Method

In each experiment, a fresh lung was obtained with the airway completely opened. The manometer was used to inflate the lung to the desired pressure. The lung was placed firmly on a tray so that when a deflection was applied to the lung, the corresponding measured resistive load would be due entirely to the tissue. The lung was kept continuously wet with saline to preserve its freshness. However, the saline was removed from the tray prior to applying a deflection (to the tissue) since water trapped beneath the lung would result in an incorrect load measurement. A polyethylene disk of (known) diameter d and negligible thickness was glued to the flat surface of the lung using Kodak Eastman 910 adhesive. Though only small deflection was applied to the lung, the disk was used to protect the lung tissue from being damaged by the probe, which would also result in faulty load measurements. The disk and adhesive used did not appreciably affect the elasticity of the lung tissue.

Figure 2.2-1. Equipment for measuring incremental Young's modulus of lung parenchyma by indentation and by flexible disk

The lung was placed underneath the deflection apparatus with the probe situated directly over the center of the disk. The reference point was determined by applying a downward deflection until the transducer just sensed a positive load. The deflection apparatus was utilized to move the probe back up to the point where the recorder indicated zero load. This was the probe's reference point: any positive deflection would result in a positive load. A known deflection (w in mm) was then applied to the center of the disk and the corresponding load (L in gm) was obtained from the recorder after a static equilibrium condition was reached. To obtain consistent results, the lung was preconditioned before applying each deflection. This also eliminated any collapsed lung tissue beneath the disk that was created by previous deflections. (As mentioned, the disk greatly reduced this effect.) For each lung, tests were run at several constant inflation pressures while the pleural pressure was kept atmospheric.

2.2.3. Data Analysis

Knowing the bulk modulus K, the other incremental moduli were then calculated using the following equations

$$\nu = A - \left(A^2 - A + \pi\right)^{1/2} \qquad A = 3\ Kwd\pi/100L \qquad (2.2\text{-}1)$$

$$E = 6K(0.5 - \nu) \qquad (2.2\text{-}2)$$

$$G = E/2(1 + \nu) \qquad (2.2\text{-}3)$$

The indentation test was performed on several rabbit and cat lungs, and on a single human lung. Typical plots of the indentation test of L versus w are shown in Figures 2.2-2 and 2.2-3. They are all extremely linear, as theory predicts for infinitesimal deformations (Hooke's Law). The values of w/L in Eq. (2.2-1) were obtained by the inverse slopes of the least squares equation given next to each plot. As expected, the slopes of these plots become steeper at higher inflation pressures because the lung becomes stiffer, and for a given deflection, the resulting resistive load of the tissue will be larger.

An average of L/w was obtained at each inflation pressure from all of the tests performed. This mean value was then used in Eq. (2.2-1) for the calculation of ν and subsequently for E and G.

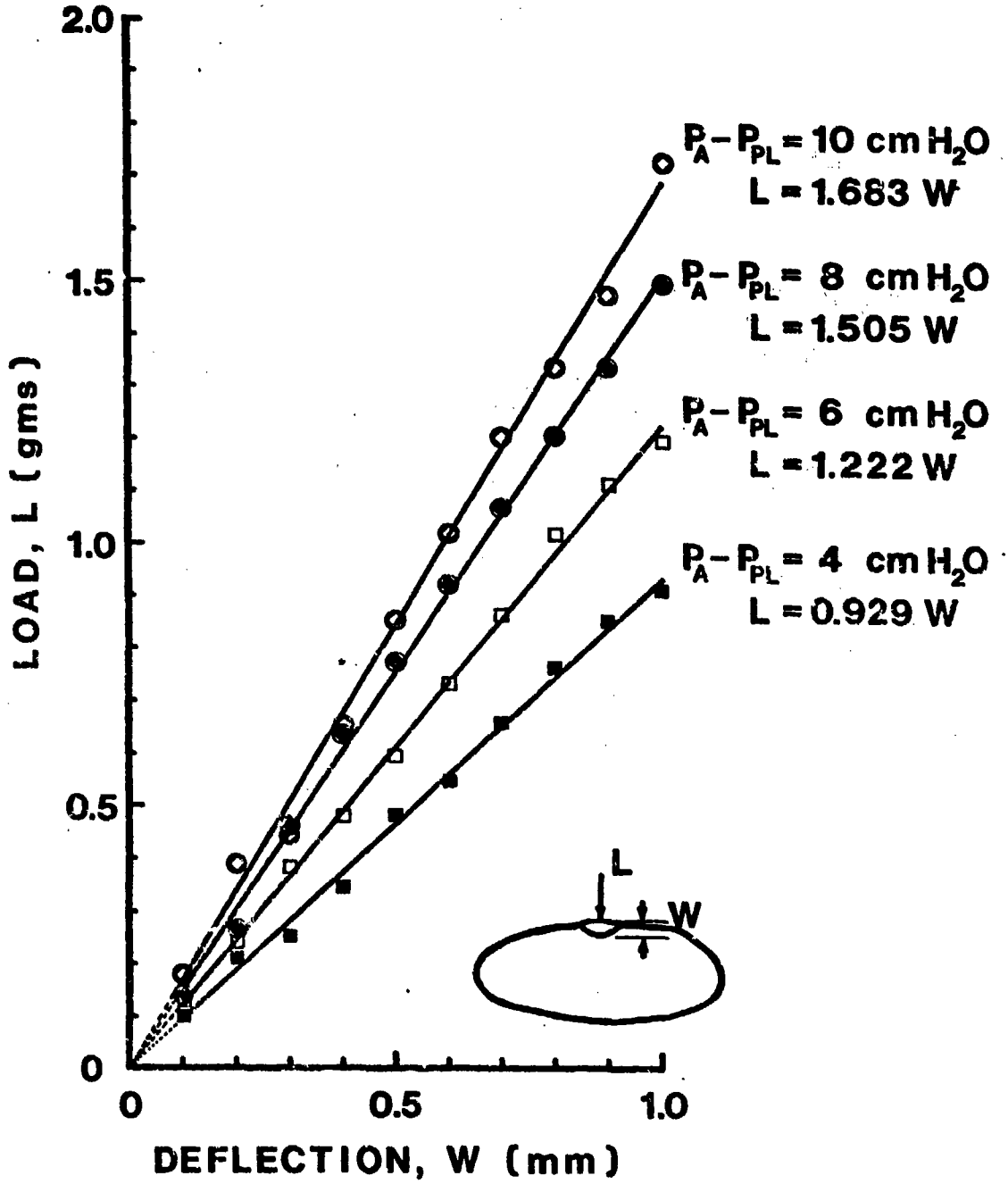

Figure 2.2-2. Experimental results on the load (L) vs deflection (w) obtained by the small-indentation method described in the text. Rabbit lungs. Equations obtained by least-squares fitting for various transpulmonary pressures ($p_A - p_{PL}$) are listed in the figure for the four cases.

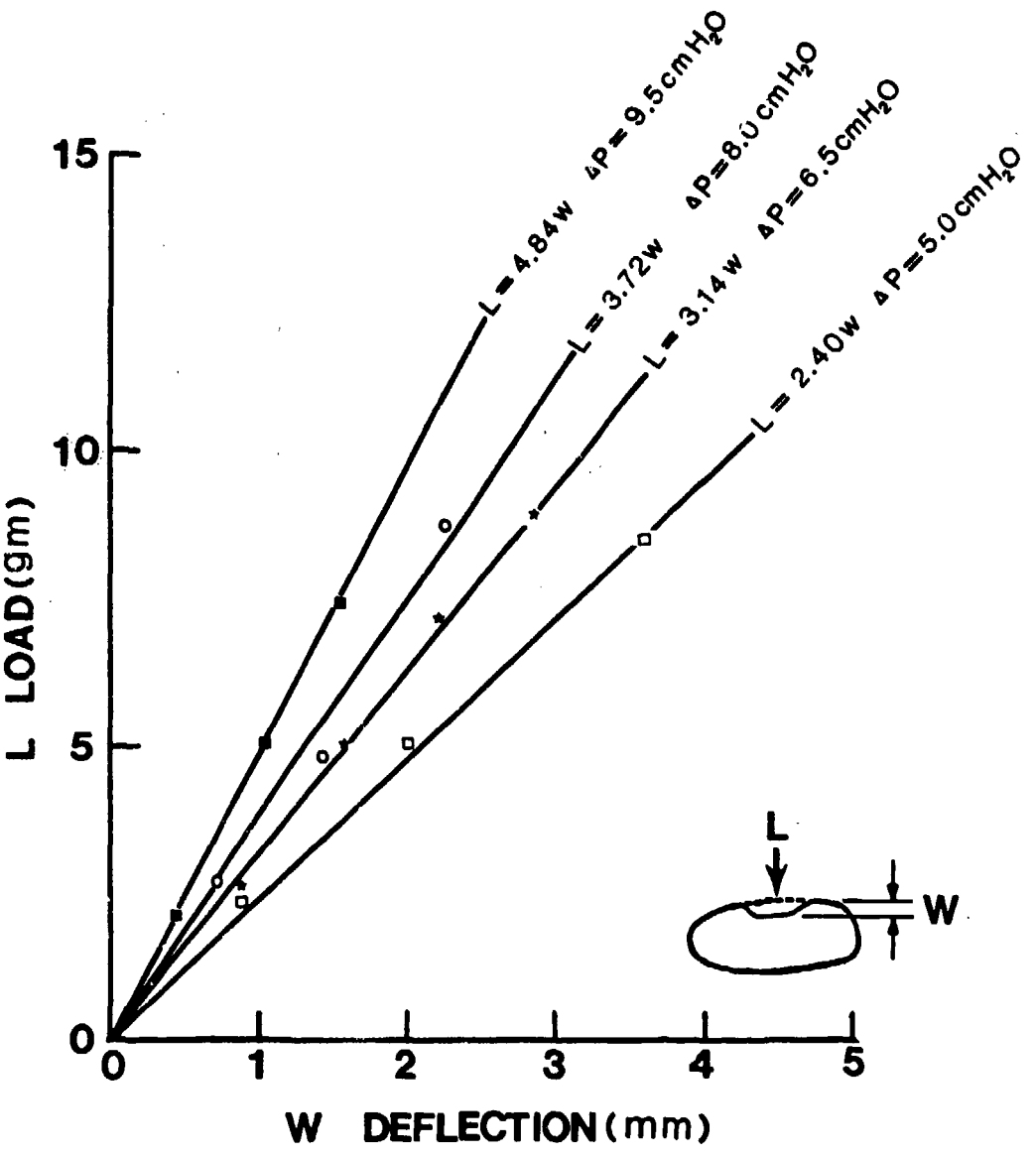

Figure 2.2-3. Typical plots resulting from small indentation test performed on a human lung for various transpulmonary pressures ($\Delta p = p_A - p_{PL}$). Equations obtained by least-squares fitting.

2.2.4. Results

Tables 2.2-1 through 2.2-3 list the calculated mean results of the incremental moduli for the rabbit, cat, and human lung, respectively. Notice that in each table the values of E and G are very constant for each inflation pressure regardless of whether the inflationary or deflationary value of K is used. Also, the values of E and G both increase with the inflation pressure, which is expected since E = stress/strain and, as previously discussed, for a given strain, the stress will be larger at higher inflation pressures. A comparison of the tables shows that the values of Young's modulus at each inflation pressure are similar for both rabbit, cat and goat lungs. Poisson's ratio for the rabbit lung varies from 0.318 to 0.400 and has a general tendency of increasing with the inflation pressure. See Figure 2.2-4. The values of ν for the cat lie in a similar range (between 0.307 and 0.405) and have a definite pattern of increasing with the inflation pressure. The values of ν for the human lung lie in a smaller, lower range between 0.276 and 0.333, and have no such definite pattern. In fact, those values of Poisson's ratio for the human lung corresponding to the deflationary values of the bulk modulus actually decrease with increasing inflation pressure.

2.3 LARGE DEFORMATION STRESS-STRAIN RELATIONS

Experiments were done to determine the mechanical properties of human lung parenchyma under large deformation. The tissue is subjected to large deformation. Rectangular slabs of human lung tissue 3 × 3 × 0.4 cm in size were cut from frozen saline-filled post mortem lungs from persons 17-41 years of age. The slabs were subjected to biaxial loading, with displacement in one direction varying sinusoidally with time while that in the perpendicular direction being kept constant. The resulting deformations were monitored continuously in the center of the specimen by video dimension analyzers. All force and displacement data were recorded digitally on-line by a PDP 11/03 computer. The specimens were soaked in normal saline at 37°C and pH 6.3, 7.25, and 7.4. The resulting stress-strain curves were highly non-linear. Viscoelastic features of hysteresis, creep and relaxation were observed. Hysteresis of the tissue in cyclic loading changed only to a minor extent when the strain rate was varied. The concept of quasilinear viscoelasticity and pseudoelasticity (Fung, 1972) seems applicable to the experimental data obtained. An

Table 2.2-1. The Incremental Young's Modulus, Poisson's Ratio and Shear Modulus of Rabbit Lung Parenchyma

	Trans-pulmonary Pressure $P_A - P_{PL}$ (cm H_2O)	n	E (cm H_2O)		Poisson's Ratio ν		G (cm H_2O)	
			Mean	S.D.	Mean	S.D.	Mean	S.D.
Inflation	4	4	12.719	0.770	0.363	0.009	4.666	0.282
Deflation	4	4	12.794	0.439	0.338	0.006	4.781	0.164
Inflation	6	4	16.659	0.398	0.376	0.003	6.053	0.145
Deflation	6	4	16.883	0.213	0.318	0.002	6.405	0.081
Inflation	8	4	20.527	1.153	0.376	0.006	7.459	0.419
Deflation	8	4	20.551	0.696	0.371	0.004	7.495	0.254
Inflation	10	4	22.882	0.837	0.389	0.004	8.237	0.301
Deflation	10	4	22.819	0.888	0.400	0.004	8.150	0.317

Table 2.2-2. Incremental Elastic Moduli for Lung Tissue of Cat

	Transpulmonary Pressure $P_A - P_{PL}$ (cm H_2O)	n	E (cm H_2O) Mean	E (cm H_2O) S.D.	ν (cm H_2O) Mean	ν (cm H_2O) S.D.	G (cm H_2O) Mean	G (cm H_2O) S.D.
Inflation	4	3	13.71	0.08	0.351	0.027	9.26	0.13
Deflation	4	3	13.84	0.10	0.307	0.038	9.04	0.20
Inflation	6	3	19.00	0.06	0.401	0.012	13.31	0.07
Deflation	6	3	19.13	0.11	0.375	0.023	13.15	0.14
Inflation	8	3	27.78	0.10	0.405	0.014	19.52	0.12
Deflation	8	3	27.85	0.18	0.395	0.024	19.43	0.21

Table 2.2-3. Incremental Elastic Moduli for Lung Tissue of Human

	Transpulmonary Pressure $P_A - P_{PL}$ (cm H_2O)	E (cm H_2O)	ν (cm H_2O)	G (cm H_2O)
Inflation	5	22.15	0.296	8.55
Deflation	5	21.98	0.333	8.24
Inflation	6.5	29.26	0.276	11.47
Deflation	6.5	29.11	0.309	11.12
Inflation	8	34.57	0.280	13.50
Deflation	8	34.30	0.301	13.18
Inflation	9.5	35.84	0.298	13.81
Deflation	9.5	38.98	0.282	15.20

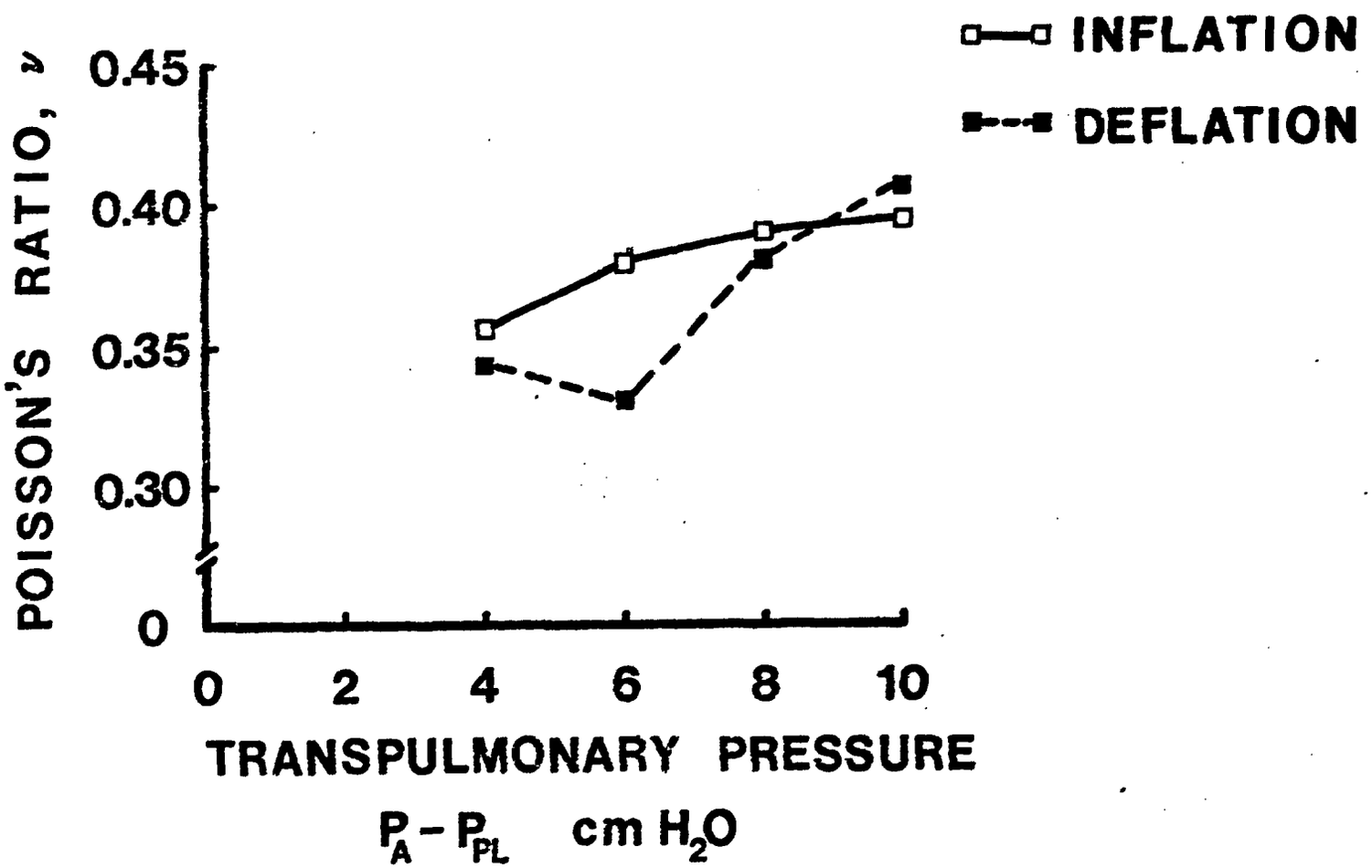

Figure 2.2-4. The relationship between the Poisson's ratio and the transpulmonary pressure ($p_A - p_{PL}$) for rabbit lungs in inflation and deflation processes

exponential pseudo-strain energy function proposed by Fung (1975) was used to describe the experimental results. The material constants obtained are compared with those of the dog's lung given by Vawter et al. (1978). The variation of these material constants with age was not significant.

2.3.1. Introduction

For the analysis of the stress and strain in the lung subjected to static and dynamic loading, it is necessary to know the mechanical properties of the lung tissue. Collection of a basic set of data on the mechanical properties is a prerequisite for dynamic analysis. Two types of data exist in the literature. In one, the lung is first inflated uniformly and then a small perturbation is imposed on it. In the other, the lung is subjected to various types of finite deformation. In the former, the incremental stresses are linearly related to the incremental strain; and experiments and data reduction are simple. In the latter, the stress-strain-history relationship is much more complicated. Depending on the applications, however, both types of data are important.

In this section, results from experiments on the human lung are presented in which the lung tissue was subjected to large deformation in a "biaxial" loading condition, and data on the stress-strain relationship, hysteresis, strain rate effect, relaxation, and creep were obtained. A constitutive equation is presented, and the material constants are identified.

2.3.2. Materials and Methods

Human lungs were obtained at autopsy less than 48 hours post mortem from patients whose cause of death did not produce an abnormality in the lung. Following excision, pressure-volume curves using air were obtained for each lung. Three of the lungs were then degassed as follows. The main bronchus of each lung was cannulated and connected to a vacuum source. The lung was then hung inside an airtight vacuum chamber containing water and maintained at a pressure of about -34 cm H_2O which corresponds to the saturation vapor pressure of water. The vacuum source connected to the bronchi was adjusted to a pressure of 1-2 cm H_2O. Thus the transpulmonary pressure was 36 cm H_2O. Each lung was subsequently slowly degassed. Following degassing they were submerged in saline and allowed to be filled via the bronchus until an equilibrium configuration was reached. Two other lungs were not degassed, but were allowed to

collapse and then filled with saline under a slight positive pressure. The liquid-filled lungs were then frozen for cutting. Slabs of lung tissue were cut 4-5 mm thick using a bandsaw, from which specimens about 3 × 3 × 0.4 cm in size were obtained.

Once cut for testing, each slab of lung tissue was allowed to thaw and its thickness measured using a tissue micrometer at a minimum of five points about the specimen surface. Only those specimens of reasonably even thickness were tested. Specimens cut from lungs which had not been degassed before saline filling and freezing were subsequently placed in a vacuum chamber for 1-2 hours for degassing before testing. Eight loops of surgical silk were sewn to each of the four edges of the specimen. Silk strings were then used to tie the loops to the force bridges of the experimental apparatus. The apparatus, nicknamed TRIAX, is a servo-controlled optical-electromechanical device described in detail by Vawter, et al. (1978). In order to avoid the edge effects introduced by this hooking system, a rectangular target was painted in the center of the specimen using titanium dioxide powder (with a carbon black border for contrast) from which displacements were monitored with video dimension analyzers. This target occupied roughly 7% of the specimen's surface area. At all times during testing the specimen was immersed in a circulating saline bath kept at 37°C. The salinity was maintained by dripping distilled water as needed. The pH of the solutions was 6.3, 7.25 and 7.4.

Stress-strain curves for slabs of human lung parenchyma were obtained as follows. Using the capability of the TRIAX to control either the force or the displacement in x and y directions, we maintained a constant force level in one direction and a displacement varying sinusoidally with time in the other direction. The amplitude of the sine wave in displacement was adjusted to produce a maximum stress of 60-70 gm/cm^2 in the direction of stretch and a minimum of about 0. The frequency was 0.4 Hz. Four levels of constant force in the opposite direction corresponding to 5, 10, 20 and 30 gm/cm^2 stress were chosen, representing roughly 7-50% of the maximum cyclic stress in the perpendicular direction. These stresses are based on the undeformed dimensions of the specimen and are therefore defined in the Lagrangian sense. As with virtually all soft tissues, lung parenchyma must be preconditioned before each test in order to obtain reproducible results. In our testing, a steady state was reached within ten cycles, with data being collected on the last cycle by

digital sampling using a PDP 11/03 computer. All loads on the specimen were released after each test so as to avoid creep over long periods of time. At various times the test in which the lateral load was held constant at a stress level of 5 gm/cm^2 was repeated so that the repeatibility of the measurements could be assessed. Anisotropy is assessed by the experimental data, and also by repeated testing with the role of x and y interchanged.

2.3.3. Experimental Results

A typical stress-strain curve for the case σ_x = 20 gm/cm^2 is shown in Figure 2.3-1. The curve is highly nonlinear, having shallow slopes for small strains and much steeper slopes for large strains. A hysteresis loop is seen. The stress-strain relationship in loading is not the same as that in unloading. But we shall see later (Figure 2.3-5) that the hysteresis loop is rather insensitive to the strain rate, and thus the loading curve and unloading curve are individually repeatable in cyclic loading. Henceforth in examining the effects of other parameters, only the loading curves will be considered.

In Figure 2.3-2, the effect of lateral tension on the stress-strain relationship (loading curves) of σ_y vs λ_y is shown. The lateral load was held constant at 5, 10, 20, 30 gm/cm^2. It is seen that the higher σ_x is, the higher the stress σ_y at any given λ_y. The curves in Figure 2.3-3 illustrate the variation among biological specimens. Here the σ_y vs λ_y curves for five specimens when σ_x was fixed at 20 gm/cm^2 are shown. Notice that λ_y ranged from 1.73 to 1.82 when σ_y was 63 gm/cm^2; whereas σ_y ranged over 40 to 62 gm/cm^2 when λ_y = 1.7. In Figure 2.3-4 the lateral displacements for tests shown in Figure 2.3-2 are exhibited. When a larger lateral force is applied, the area of the hysteresis loop is smaller.

To assess the effects of strain rate on the stress-strain relationship, the rate of stretch was varied over 20-fold (the cycle time was varied from 25 to 500 s). The results are shown in Figure 2.3-5. It is seen that the stress-strain relationship of human lung tissue is rather insensitive to strain rate.

2.3.4. Relaxation and Creep

In Figure 2.3-6 some typical relaxation curves of human lung tissue subjected to a step-change in strain are plotted. It is seen that the relaxation phenomenon is significant for the lung tissue, especially at higher levels of

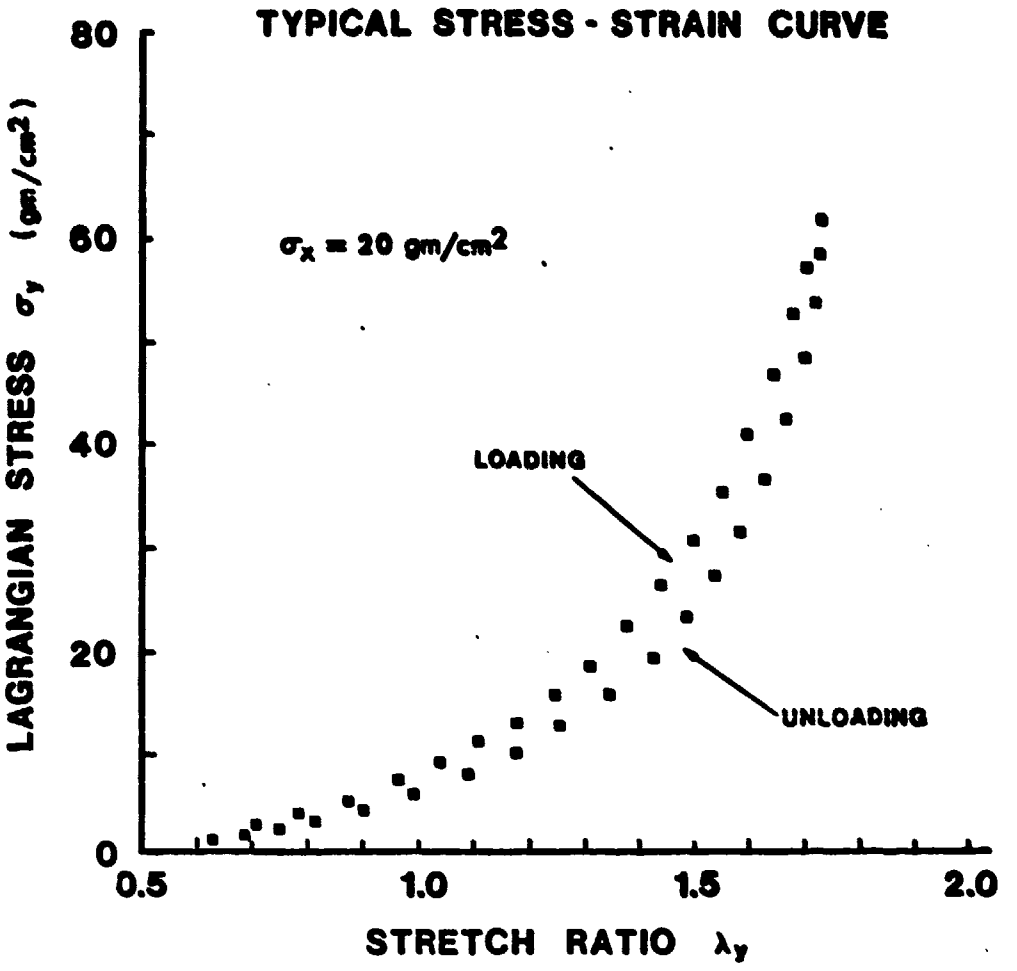

Figure 2.3-1. A typical stress-strain curve

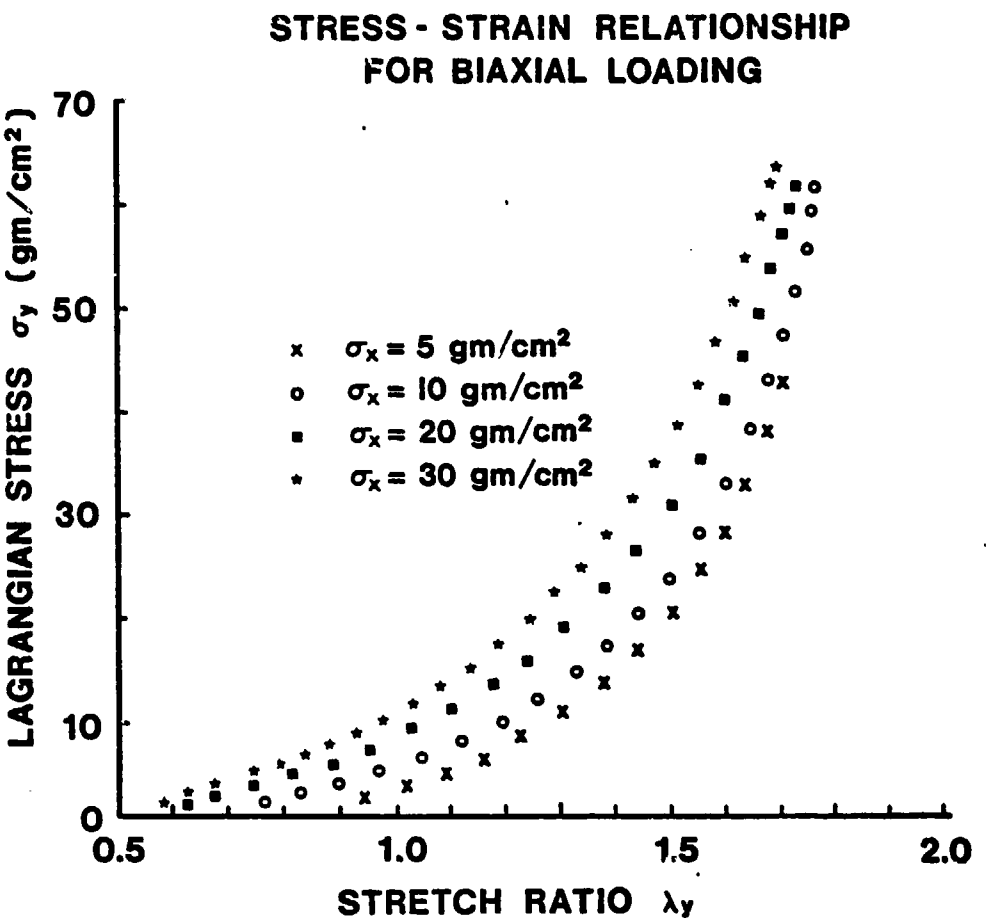

Figure 2.3-2. Stress-strain curves of σ_y vs λ_y when σ_x was held at various fixed values

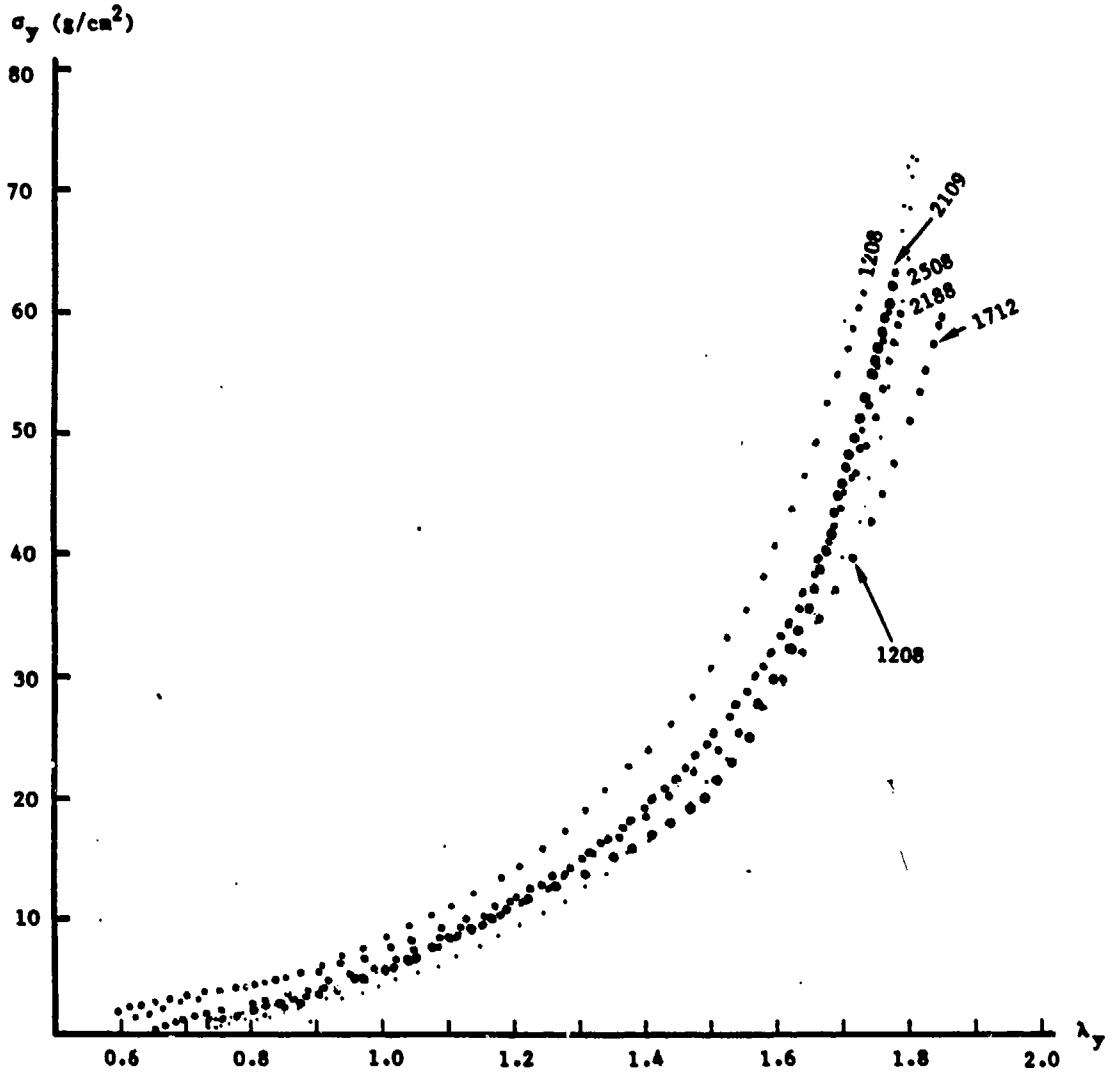

Figure 2.3-3. Loading stress-strain curves for 5 specimens (σ_x = 20g/cm^2)

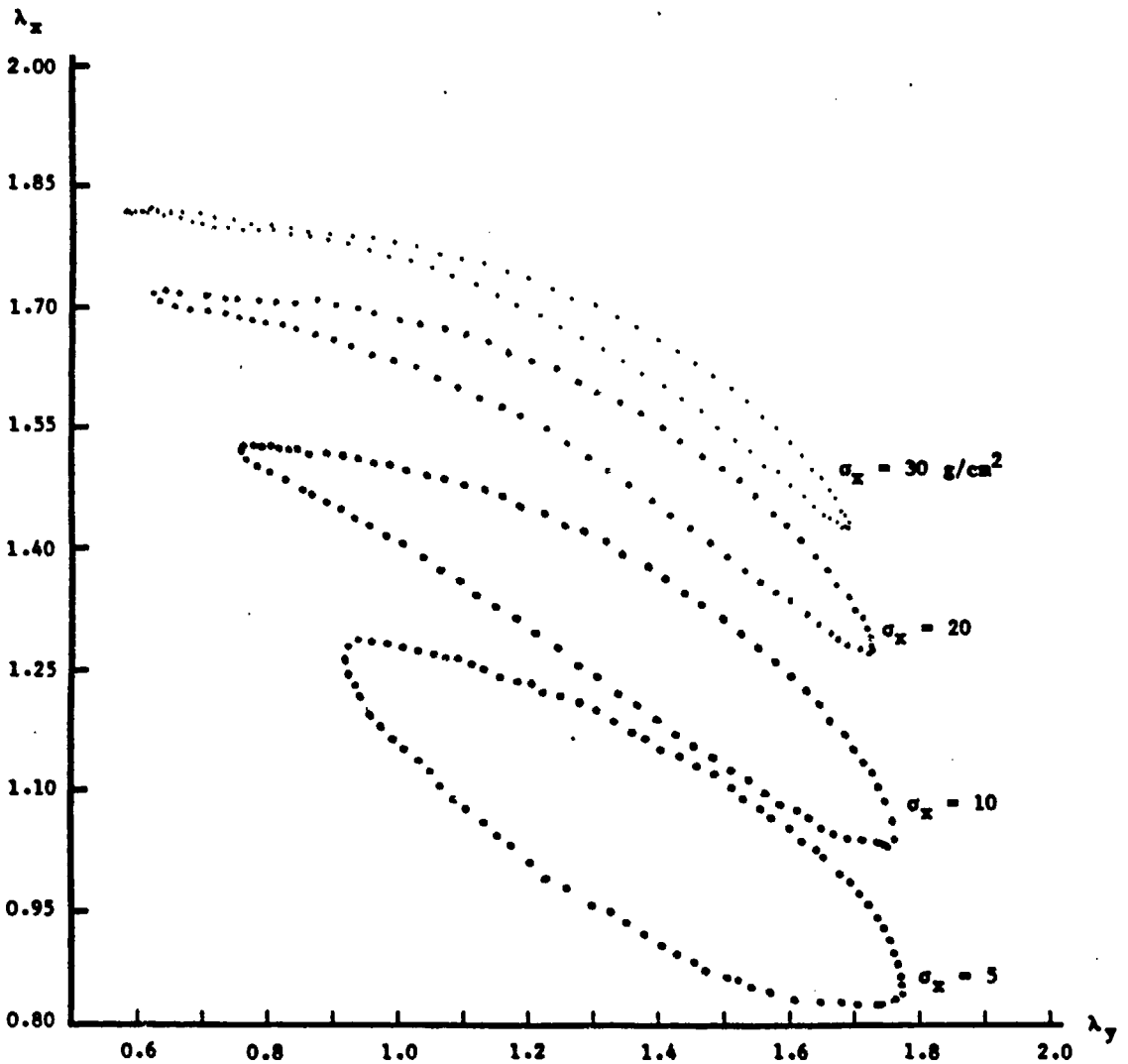

Figure 2.3-4. Lateral displacement

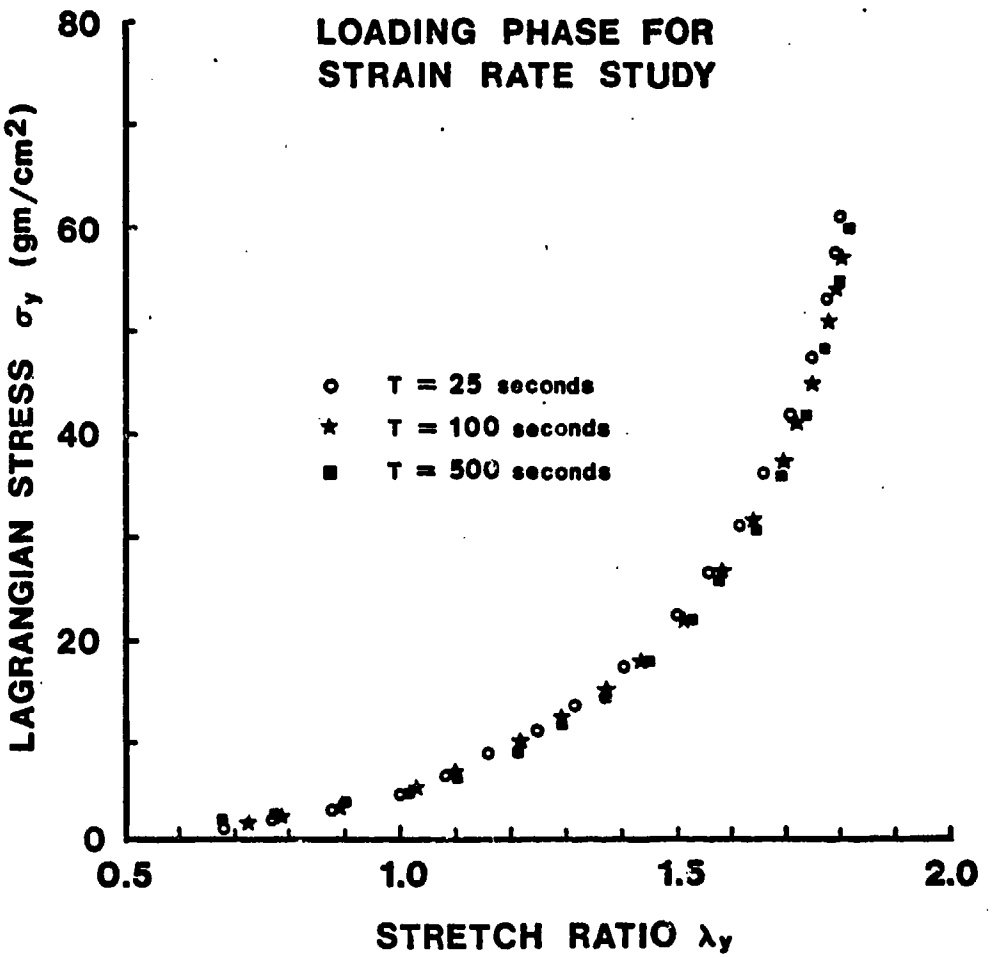

Figure 2.3-5. Stress-strain relationship σ_y vs λ_y measured at various strain rates

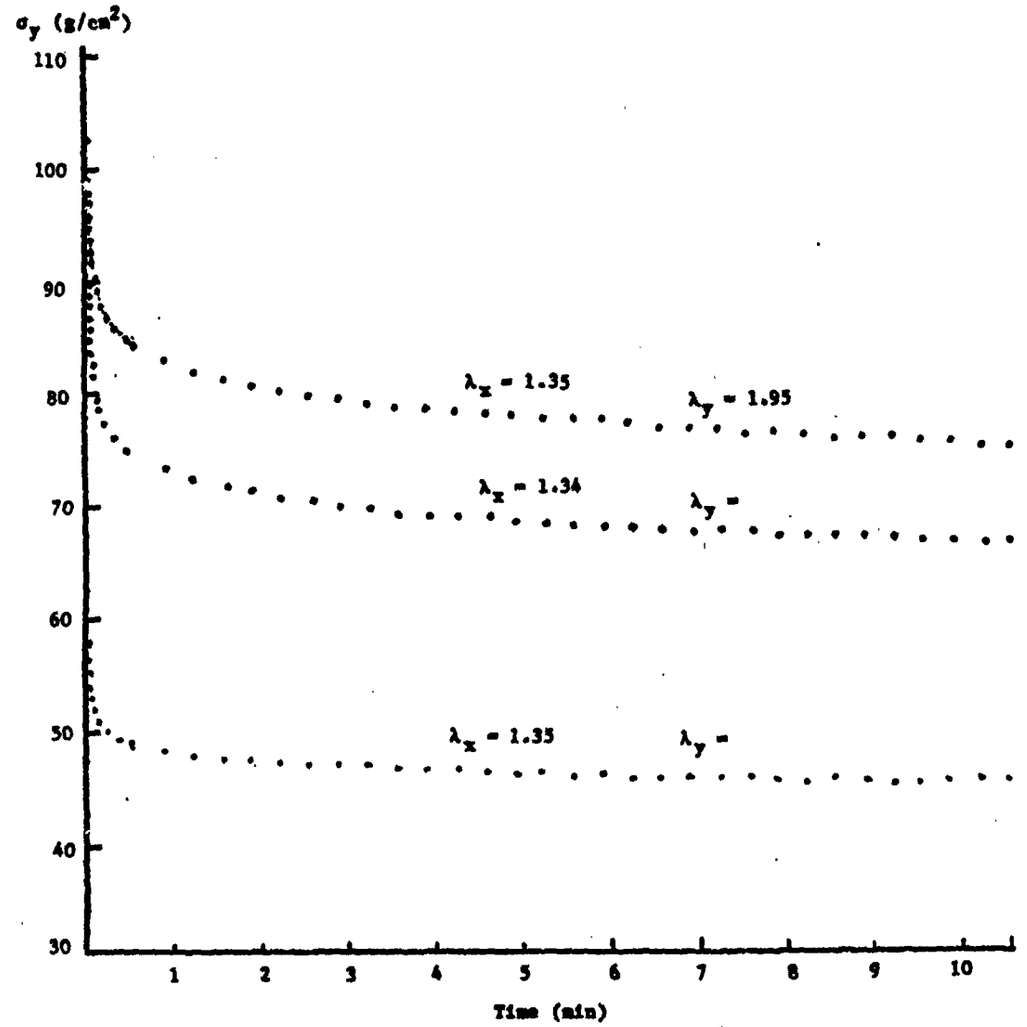

Figure 2.3-6. Relaxation of human lung tissue

strain. Figure 2.3-7 shows the results on a logarithmic time scale that reveals the various periods.

Figure 2.3-8 shows the creep curves of the lung tissue under constant loads. It is seen that creep in the lung exists, but is remarkably small.

2.3.5. The Constitutive Equation

A mathematical expression describing the mechanical properties of a material is called the constitutive equation. The mechanical behavior of human lung tissue exhibited in Figures 2.3-1 through 2.3-8 is fairly similar to that of some other soft tissues so that the constitutive equation suggested by Fung (1975, 1981) seems applicable. This constitutive equation is based on the concept of quasi-linear viscoelasticity and pseudo-elastic strain energy. Expressed in the form of a pseudo strain energy function, we have:

$$\rho_o W = \frac{1}{2} C \exp[a_1 E_x^2 + a_2 E_y^2 + 2a_4 E_x E_y] + \begin{matrix}\text{symmetric terms obtained} \\ \text{by permuting x, y, and z}\end{matrix} \qquad (2.3\text{-}1)$$

where ρ_o is the density of the lung in the reference state, W is the pseudo strain energy per unit mass, and C, a_1, a_2, a_4 are material constants. E_x, E_y are Green's strains which are related to the stretch ratios λ_x and λ_y as follows:

$$E_x = (\lambda_x^2 - 1)/2 \quad , \qquad E_y = (\lambda_y^2 - 1)/2 \quad . \qquad (2.3\text{-}2)$$

Hence, we have the Lagrangian stresses

$$\sigma_x = \frac{\partial(\rho_o W)}{\partial \lambda_x} = C\,\lambda_x(a_1 E_x + a_4 E_y)\exp[a_1 E_x^2 + a_2 E_y^2 + 2a_4 E_x E_y]$$

$$+ C\,\lambda_x(a_1 E_x + a_4 E_z)\exp[a_1 E_x^2 + a_2 E_z^2 + 2a_4 E_x E_z] \quad , \qquad (2.3\text{-}3a)$$

$$\sigma_y = \frac{\partial(\rho_o W)}{\partial \lambda_y} = C\lambda_y(a_2 E_y + a_4 E_x)\exp[a_1 E_x^2 + a_2 E_y^2 + 2a_4 E_x E_y]$$

$$+ C\lambda_y(a_2 E_y + a_4 E_z)\exp[a_1 E_z^2 + a_2 E_y^2 + 2a_4 E_z E_y] \quad . \qquad (2.3\text{-}3b)$$

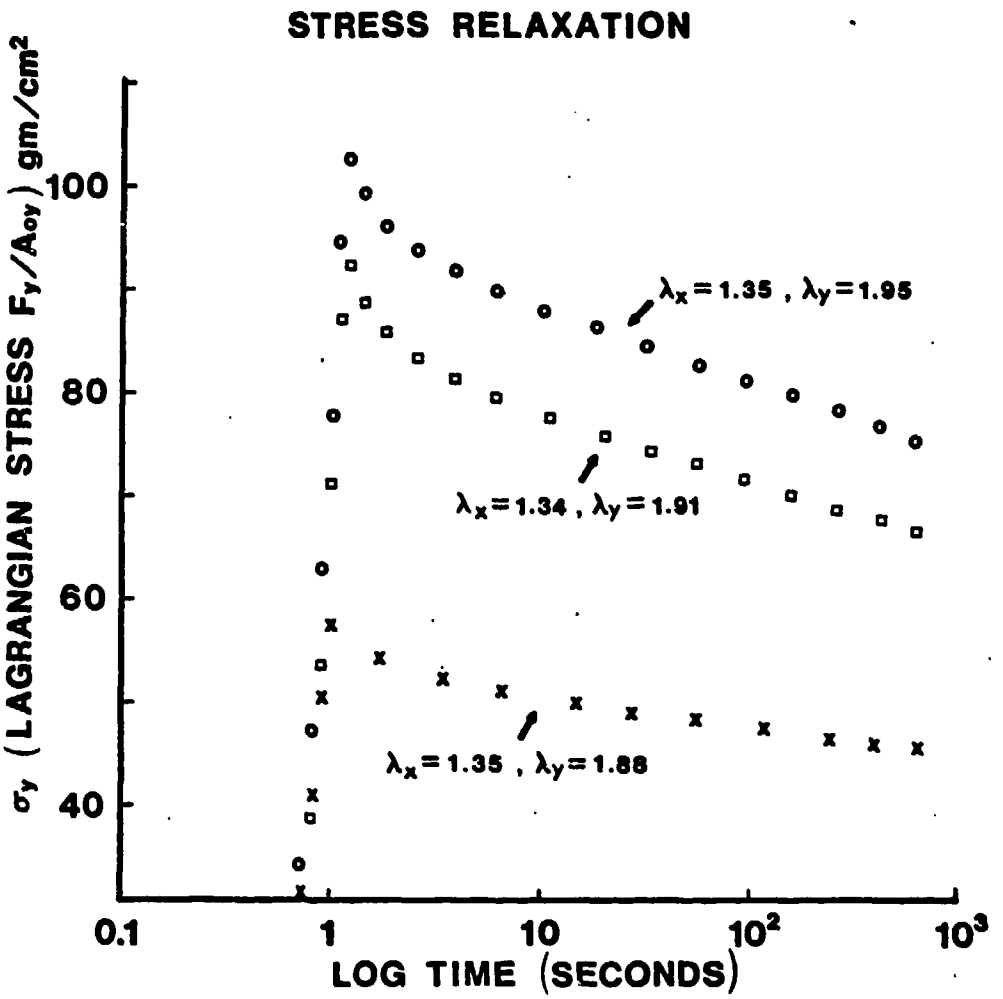

Figure 2.3-7. Relaxation of human lung tissue

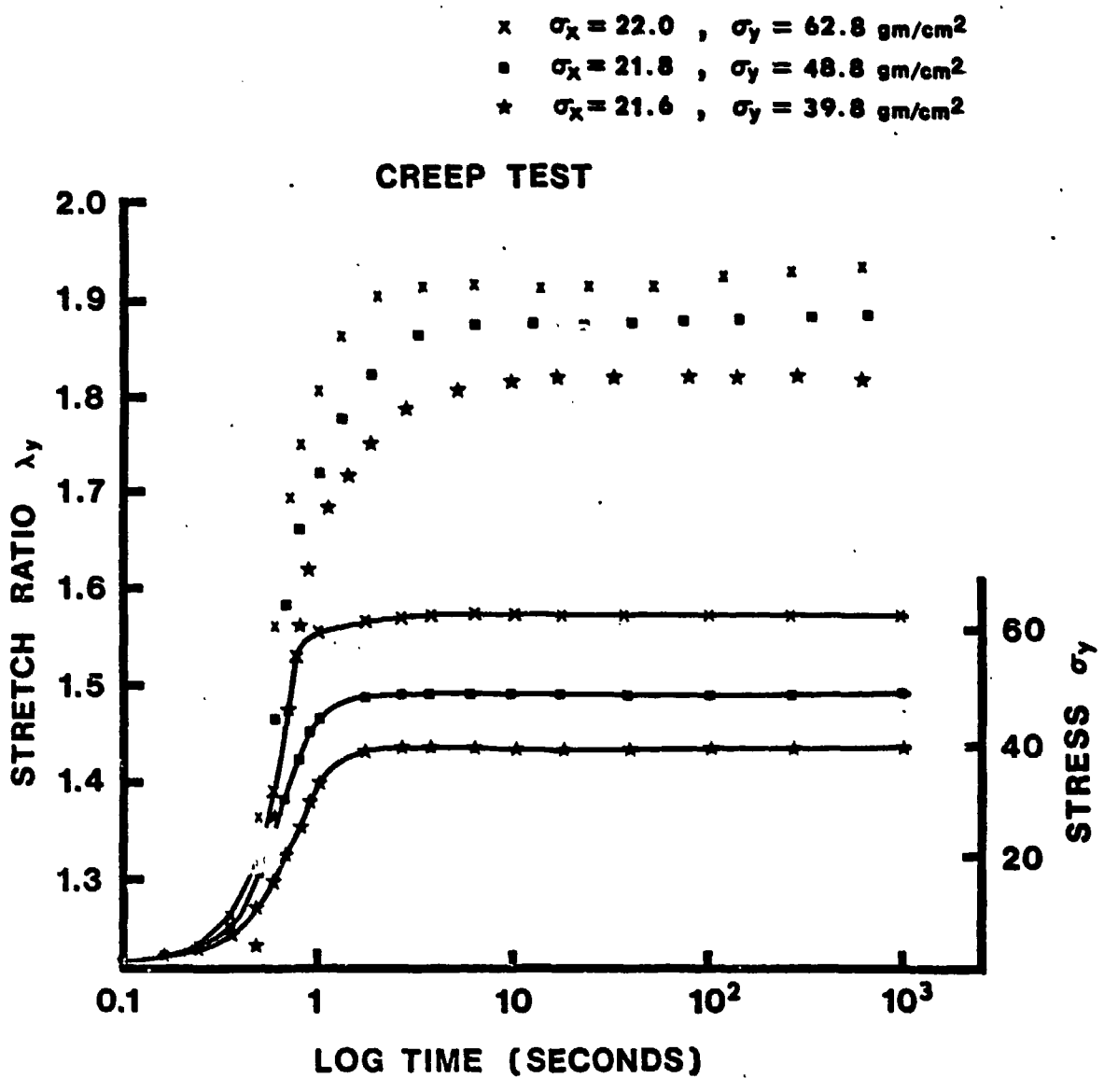

Figure 2.3-8. Creep of human lung tissue

Equations (2.3-3) show that the constant C determines the overall stress level, whereas a_1 and a_2 determine the range of change of stress with increasing stress, and a_4 determines the coupling between two perpendicular directions. If the lung parenchyma is assumed to be isotropic in the reference state, then a_1 and a_2 are equal. Hence, for initially isotropic lung tissue,

$$\sigma_x = C\lambda_x(a_1E_x + a_4E_y)\exp[a_1(E_x^2 + E_y^2) + 2a_4E_xE_y]$$
$$+ C\lambda_x(a_1E_x + a_4E_z)\exp[a_1(E_x^2 + E_z^2) + 2a_4E_xE_z] \quad , \qquad (2.3\text{-}4a)$$

$$\sigma_y = C\lambda_y(a_1E_y + a_4E_x)\exp[a_1(E_x^2 + E_y^2) + 2a_4E_xE_y]$$
$$+ C\lambda_y(a_1E_y + a_4E_z)\exp[a_1(E_z^2 + E_y^2) + 2a_4E_zE_y] \quad . \qquad (2.3\text{-}4b)$$

When experimental values of σ_x, σ_y, E_x, E_y, E_z are substituted into Eqs. (2.3-3) and (2.3-4), we can identify the material constants C, a_1, a_2, and a_4 by minimizing the sum of the squares of errors between experimental and computed stresses.

2.3.6. Material Constants

Five human lungs have been tested, as listed in Table 2.3-1. All test specimens are tested at 37°C. Two (1712, 2111) were tested at pH = 7.4, two (2508, 1208) at pH = 6.3, and one (2109) at pH = 7.25. For each specimen, one hundred data points were recorded in the computer. These are used to identify the material constants.

Our results are presented in Tables 2.3-2 and 2.3-3. The material constants are listed separately for the loading and unloading conditions, and under the assumptions of isotropy or anistropy. In general, the fitting between the constitutive equation and the experimental data is very good.

Table 2.3-1. Identification of Human Lung Specimens

Specimen Number	Age	Sex
1712	41	Male
2111	24	Male
2508	21	Male
2109	28	Male
1208	17	Male

Table 2.3-2. Mean Values of Lung Elasticity Material Constants in Loading Process

a. Lung Tissue Considered Anisotropic

Specimen No.	T°C	pH	C±S.D. (g/cm^2)	a_1±S.D.	a_2±S.D.	a_4±S.D.
1712	37	7.4	5.84±1.19	0.80±0.26	0.75±0.12	0.53±0.14
2111	37	7.4	8.57±3.19	0.68±0.24	0.71±0.14	0.44±0.14
2508	37	6.3	4.57±1.48	1.60±1.54	1.00±0.25	0.73±0.50
2109	37	7.25	8.75±3.46	0.54±0.12	0.73±0.17	0.37±0.07
1208	37	6.3	10.32±2.90	0.53±0.16	0.73±0.13	0.47±0.11
Mean:			7.57±2.33	0.83±0.44	0.78±0.12	0.51±0.14

b. Lung Tissue Considered Isotropic

Specimen No.	T°C	pH	C±S.D. (g/cm^2)	$a_1 = a_2$±S.D.	a_4±S.D.
1712	37	7.4	5.21±0.78	0.78±0.02	0.53±0.07
2111	37	7.4	5.52±0.90	0.86±0.07	0.51±0.05
2508	37	6.3	3.92±2.15	1.11±0.33	0.63±0.17
2109	37	7.25	3.80±4.01	1.16±0.39	2.63±0.19
1208	37	6.3	3.13±2.89	1.40±0.41	0.91±0.24
Mean:			4.32±1.01	1.06±0.25	0.64±0.16

Table 2.3-3. Mean Values of Lung Elasticity Material Constants in Unloading Process

a. Lung Tissue Considered Anisotropic

Specimen No.	T°C	pH	C±S.D. (g/cm^2)	a_1±S.D.	a_2±S.D.	a_4±S.D.
1712	37	7.4	4.01±0.49	1.22±0.57	0.89±0.18	0.82±0.36
2111	37	7.4	4.54±1.82	1.23±0.57	0.98±0.20	0.68±0.26
2508	37	6.3	3.40±1.38	1.42±0.71	1.12±0.27	0.75±0.35
2109	37	7.25	4.83±1.52	0.83±0.27	0.93±0.19	0.52±0.11
1208	37	6.3	6.07±1.24	0.78±0.23	0.94±0.16	0.63±0.15
Mean:			4.57±1.00	1.10±0.28	0.97±0.09	0.68±0.11

b. Lung Tissue Considered Isotropic

Specimen No.	T°C	pH	C±S.D. (g/cm^2)	$a_1 = a_2$±S.D.	a_4±S.D.
1712	37	7.4	4.93±1.26	0.82±0.22	0.70±0.29
2111	37	7.4	4.30±0.73	0.97±0.12	0.61±0.12
2508	37	6.3	3.89±1.40	1.04±0.29	0.65±0.23
2109	37	7.25	2.70±1.29	1.15±0.17	0.65±0.07
1208	37	6.3	3.30±1.52	1.21±0.12	0.86±0.12
Mean:			3.82±0.86	1.04±0.15	0.69±0.10

3. WAVE PROPAGATION IN THE LUNG*

3.1 INTRODUCTION

Because of the relatively slow speed of stress waves in the lung, the features of wave reflection, focusing, and interaction often dominate the scene of lung dynamics in response to impact loading. In any attempt to analyze the lung dynamics, it is necessary to know the speed of wave propagation. In the past, Clemedson and Jönsson (1962) have measured the wave speed in the lung by inserting two pressure transducers (of diameter 3/32 inch or 2.38 mm) into the airways of the right and left lungs of an anesthetized rabbit or calf and then subjected the animal to an air shock wave. By measuring the difference of the arrival times of the stress waves at the probes and the distance between the probes by autopsy, they obtained the velocity of the main part of the pressure pulse in the calf lungs inflated to approximately intravital size to be between 24 and 30 m/sec. For rabbit lungs they found speeds of 15, 32, and 69 m/sec in several animals but considered the data as uncertain. In collapsed rabbit lung they found a wave speed of 15 m/sec. Rice (1983), using a microphone and a spark gap sound source, measured the transit time of sound through the lung and estimated the sound speed in air-filled excised horse lung to be between 25 and 70 m/sec, depending on lung volume. Dunn and Fry (1961), using reflection coefficient for ultrasound energy and the density of the lung tissue, calculated a wave speed of 650 m/sec. These are the data in the literature as far as we know.

The lung has a complex structure and the lung parenchyma is a composite material with a highly nonlinear stress-strain relationship. Many types of waves can exist in it. Which one is excited depends on the mode of excitation and the amplitude of the loading. The 10- to 20-fold difference between the data quoted above reflects the fact that different kinds of waves were excited in different experiments. It follows that one should design one's experiment according to the intended application, so that the type of the impact load and its amplitude level can be properly chosen. In the present study, we are

*By M. R. Yen, Y. C. Fung, H. H. Ho, and G. Buttermann

interested in the dynamics of the lung in response to impact or shock wave acting on the chest; hence the impact load level should be relevant to the problem of possible lung injury. In the following we present the results of our measurement of wave speed in the lungs of the rabbit, the goat, and man with a method in which a water jet was used to impose an impact load on the lung. A pressure transducer was used to record the pressure wave produced by the jet hitting the lung. The transducer was also placed at a point on the far side of the lung to sense the arrival of the stress waves. A photosensor was placed at various places between the nozzle of the water jet and the lung to measure the arrival of the water. From these signals the velocity of the water jet and the speed of the stress wave in the lung can be determined.

The objective of our study is similar to that of Clemedson and Jönsson, but different from those of Dunn and Fry and those of Rice. The impact pressure level on the surface should be in the range of 1-5 psi (7-35 kPa), and the surface velocity should be in the order of 1-10 m/sec. According to Clemedson and Jönsson (1975) severe hemorrhages in the lung are highly probable for a maximum surface velocity exceeding about 10 m/sec. We chose to use a water jet to deliver an impact in this range. The velocity, momentum and area of impact of the water jet can be controlled.

Our choice of water jet is based on the following consideration. Clemedson and Jönsson (1964) used the detonation of a high explosive in a "wave guide" (constituted of two concentric cylinders) to impose a planar shock wave on the animal. By their method the determination of the wave arrival time is difficult as can be seen from the cathode ray traces in their paper. In earlier stages of our own experiment, we designed and used several shock tubes (using compressed air and paper membrane) to produce a loading in an overpressure range of a few psi. The weak supersonic shock is followed by a bulk flow. The lung responds to both the weak supersonic shock wave and the large bulk flow, and the determination of wave propagation characteristics is often difficult. This difficulty was minimized by using the water jet.

3.2 APPARATUS

Figure 3-1 is a photograph of the test equipment used for measuring the elastic wave propagation in the lung. Figure 3-2 is a block diagram of the testing apparatus. The apparatus consists of three subgroups, the first of which is the water jet for imposing impact loading on the surface of the lung. To obtain a well defined impulse loading covering a circle of 2 mm diameter on the surface of the lung, a water jet was constructed. A fluid reservoir driven by a pressure regulated air source charged a small hydraulic accumulator through a normally open flexure electronic poppet valve. This valve, manufactured by Clippard Minimatic, has an activating time of < 3 ms due to a very low mass of flexure poppet. The valve was designed to operate at 5 volts DC at 100 mA. When a normal trigger was applied to the valve sequencer, valve A would close, isolating the accumulator from the fluid reservoir. After 30 ms the valve B, an identical flexure poppet valve, would open for 5 ms, discharging the accumulator through the nozzle. The nozzle itself consisted of 5 holes of 0.3 mm diameter each grouped in a 2 mm circle.

The second subgroup consisted of the photosensor system which was used to sense the arrival of the water jet. The photosensor could be moved with precision along the axis of the jet to calculate the velocity of the fluid in the air. The conditioning electronics incorporated a hi-pass filter with a time constant of 100 μs to eliminate ambient light effects.

The third subgroup consisted of the pressure transducer used to record the response of the lung due to water impact. The arrival time and the pressure wave were recorded. The pressure transducer was connected to a Neff amplifier and the output was shown on a Tektronix 5440 oscilloscope. The pressure transducer was an Endevco Model 8510-2 m21 with a calibrated sensitivity of 151.6 m volts/psi.

3.3 ANIMAL PREPARATION

Animals such as goats, etc. were first anesthetized using a proper dose ($\sim$ 7 mg/kg) of Nembutal. Heparin (145 units/kg) was then injected into the bloodstream to prevent blood coagulation. The trachea was cannulated. Through a midline incision of the chest, the lung was exposed and excised. An isolation of the lung lobes was then made after placing the lung in a saline filled tray.

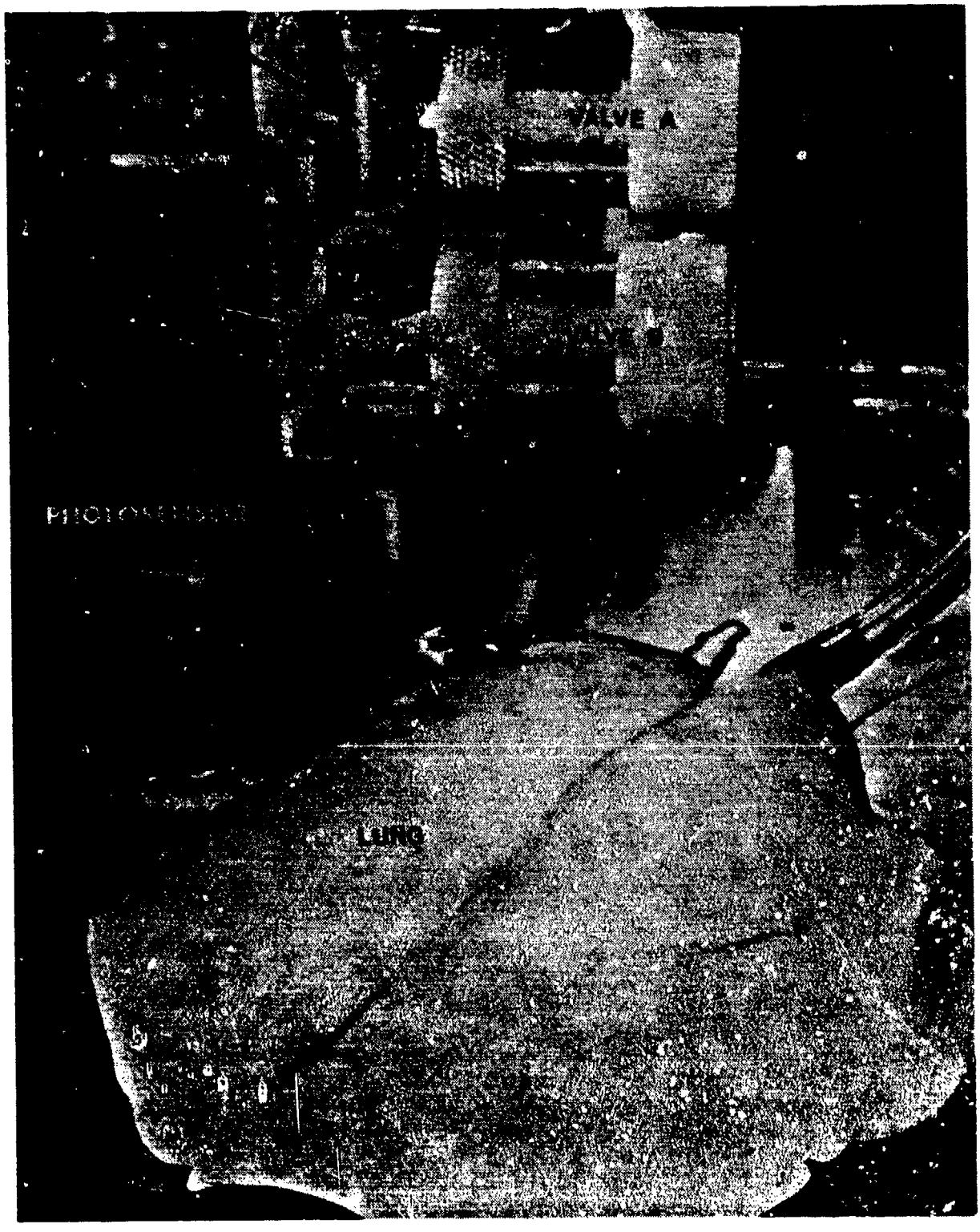

Figure 3-1. The test equipment for measuring the elastic wave propagation in the lung

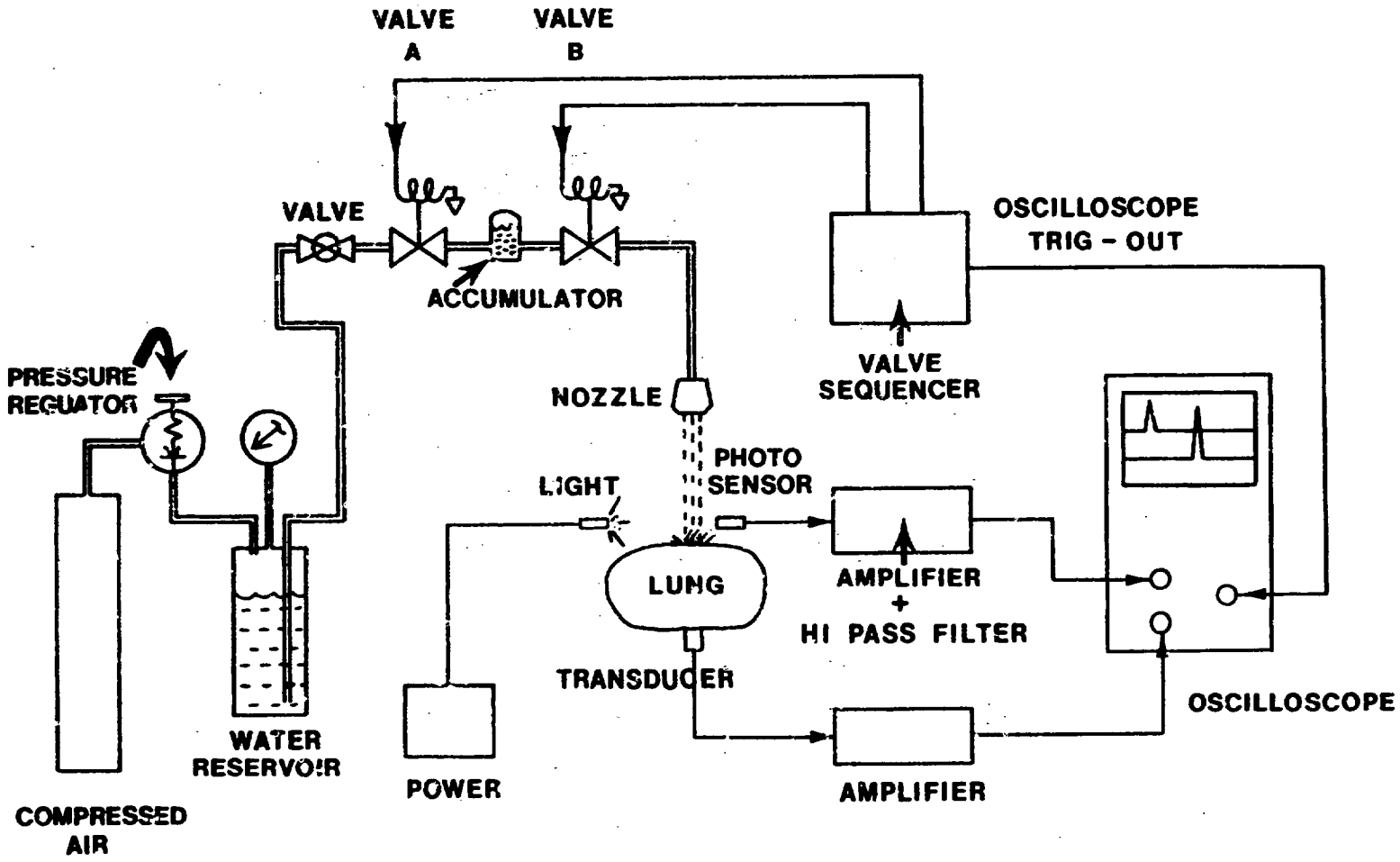

Figure 3-2. A schematic diagram of the wave propagation testing apparatus. The apparatus consists of three subgroups: water jet, photosensor system, and pressure response measuring system.

3.4 EXPERIMENTAL METHOD

The experimental protocol is shown in Figure 3-2. The lung was placed firmly on a pressure transducer in a supporting basin. A water jet was placed directly above the lung, with a distance of 1.8 cm from the bottom of the nozzle to the surface of the lung. The nozzle has five holes to allow five small jets converging onto one area on the lung surface. A photosensing tube was placed between the lung surface and the nozzle. In each experiment, the reservoir air pressure was kept constant (50-60 psi). With a touch of the control unit key, a water jet was fired. The screen of the oscilloscope showed the output. For each constant reservoir air pressure, at least three photosensor positions were used in the experiment. Then another reservoir air pressure was selected and the experiments were repeated. The airway pressures of the lung were chosen to be 0, 5, 10, 15 and 20 cm H_2O. The pleural pressure was zero (atmospheric). We then plotted on an x-y coordinate paper (Figure 3-3) the distance from the top of the pressure transducer (d) versus the difference in time (t) between the leading edges of the pressure wave and photosensor wave. For each water ejection setting (pressure in the accumulator) a straight line was obtained. By changing the setting, different straight lines were obtained. These lines would intersect at one point which marked the time and distance of the point where the water jet hit the lung surface. In this way we obtained the lung thickness d. The corresponding time t is the traveling time of impact wave in the lung tissue. Hence the wave speed of the lung tissue is $c = d/t$.

3.5 DATA ANALYSIS

Figure 3-4 shows a typical set of experimental curves. Figure 3-4(a) shows the pressure wave due to impact of the water jet on the transducer located at the place where the jet hits the lung (with the lung removed). This particular wave shows a peak pressure of 1.7 psi. Figure 3-4(b) shows the usual format of the outputs recorded on the screen of the oscilloscope. The upper curve is the response of the photosensor indicating the arrival of the water jet. The lower curve is the response of the pressure transducer which indicates the stress wave in the lung at the place where the transducer was located. The first sharp wave is used to correlate the impact wave imposed on the lung. The time difference between the arrival of the water jet on the

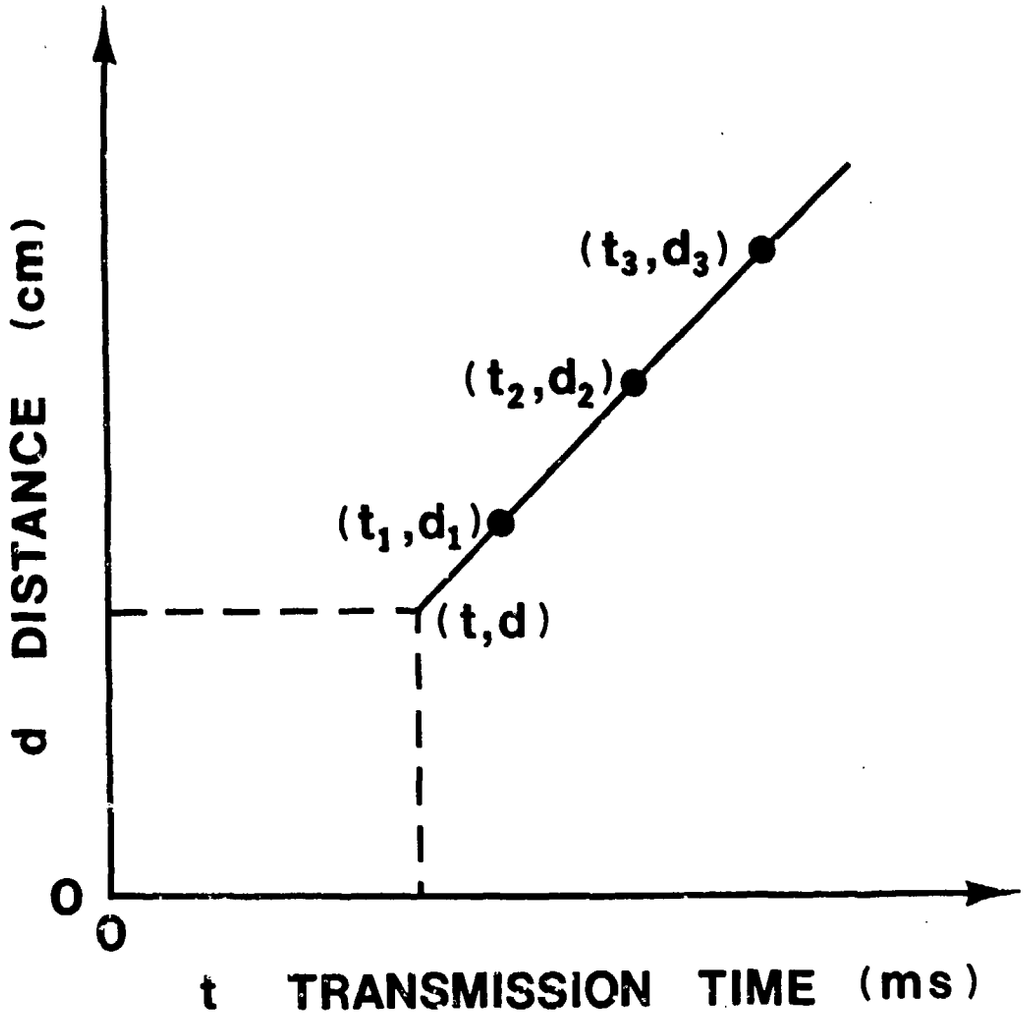

Figure 3-3. x-y plotting of the distance d versus transmission time t

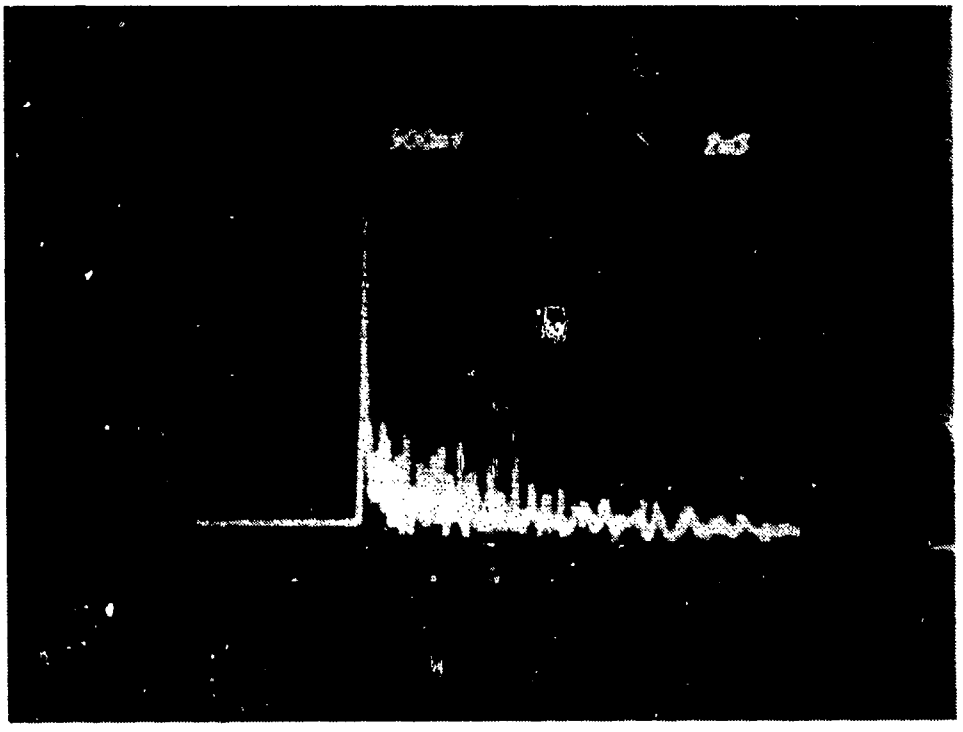

(a) The pressure transducer response due to impact of the water jet. The peak of the pulse in this example is 1.7 psi.

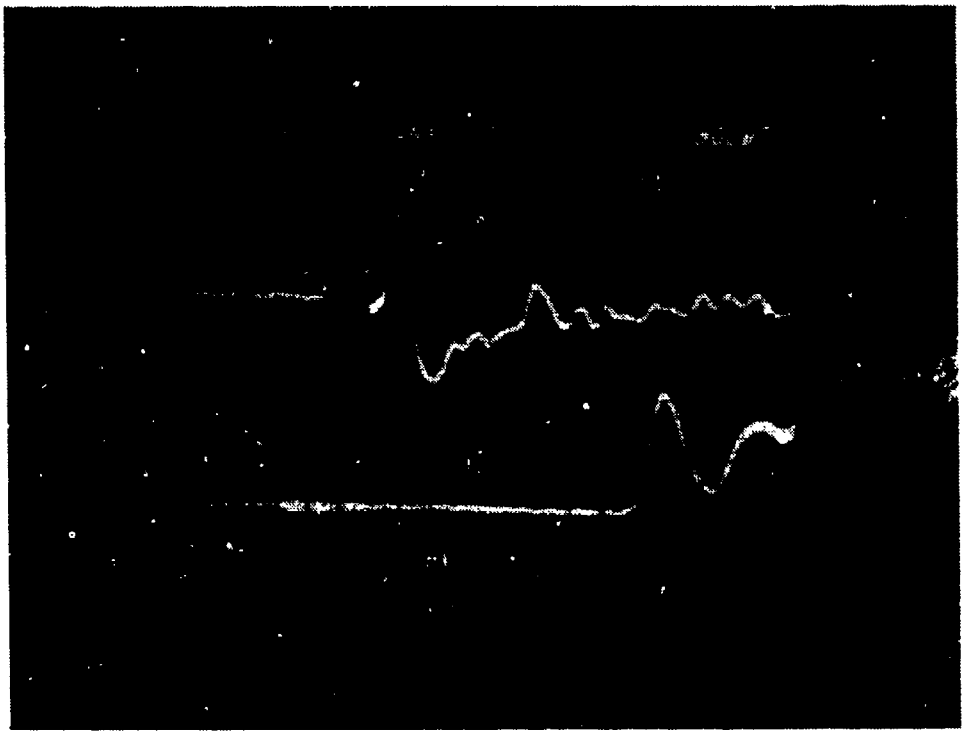

(b) Example of output response recorded on the screen of the oscilloscope. The upper curve indicates the arrival of water jet on the photosensor. The lower curve is the response of the pressure transducer which indicates the stress wave propagation. The first sharp wave is used to correlate the impact wave imposed on the lung. In this particular example, the peak is 0.003 psi according to the calibrated scale (one division is 0.0015 psi).

Figure 3-4. Typical experimental curves

photosensor and first arrival of the wave by impact was measured and designated as t_1 corresponding to photosensor position d_1; at least two other photosensor positions were chosen and the results are designated as t_2, d_2 and t_3, d_3. These data are used to obtain the water jet speed in the air (the slope of the curve) as well as the distance and traveling time in the lung tissue (Fig. 3-3).

3.6 RESULTS

Table 3-1 gives the experimental results of goat lung for several airway pressures. The values of wave speed c lie in the range of 30 to 70 m/s, and have a general pattern of increasing with the airway pressure. Here n is the number of experiments and σ is the standard deviation.

Table 3-2 summarizes the experimental results of the rabbit lung.

3.7 COMPARISON WITH DATA IN THE LITERATURE

It is often stated that the velocity of stress wave in soft tissues of the body is equal to the velocity of sound in water due to the high water content of most animal tissues [see, e.g., Corey (1946), Schardin (1950); c.f. also White and Richmond (1959)]. The data on the lung show that this is incorrect.

Table 3-3 gives the velocity of sound in various soft and hard tissues. Comparing the velocity of sound in the lung with that in other tissues, one sees at once that the wave speed is uniquely low in the lung.

3.8 DISCUSSION

The wave speed obtained from lungs with their blood drained were different from those obtained for lungs filled with blood. Usually the values for the blood-drained lungs were found to be higher. In one experiment using goat lung with no blood in the pulmonary blood vessels, the obtained values corresponding to airway pressures of 0, 5, 10, and 15 cm H_2O were 38.7 ±1.8, 52.5 ±3.0, 67.7 ± 4.9, and 77.8 ±3.7 m/sec, respectively. Compared with the previous results with blood in the pulmonary blood vessels, it is seen that these values are higher. This finding appears to be reasonable. If we consider the lung tissue to be incrementally linearly elastic, then the square of the wave

Table 3-1. Stress Wave Speed in Goat Lung p_A is Airway Pressure and p_{PL} is Pleural Pressure Which is Atmospheric

Transpulmonary Pressure $p_A - p_{PL}$	Velocity (m/s)	n	Mean Value of Wave Velocity (m/s)	Standard Deviation σ
0	31.6 30.8 31.8	3	31.4	0.4
5	32.7 33.8 31.4 37.6	4	33.9	2.3
10	37.7 37.4 36.1 32.1 37.8 35.6	6	36.1	1.9
15	46.9 43.0 46.7 48.7 47.2 48.2	6	46.8	1.8
20	66.5 64.7 58.5 69.1	4	64.7	3.9

Table 3-2. Stress Wave Speed in Rabbit Lung p_A is Airway Pressure and p_{PL} is Pleural Pressure Which is Atmospheric

Transpulmonary Pressure $p_A - p_{PL}$	Velocity (m/s)	n	Mean Value of Wave Velocity (m/s)	Standard Deviation σ
0	15.2 15.4 21.7 15.0 15.0 16.4	6	16.5	2.4
4	32.1 31.1 28.6 30.9 28.6 22.1	6	28.9	3.3
8	29.6 31.9 31.3 31.6 32.3	5	31.3	0.9
12	35.5 35.5 36.2 34.2	4	35.3	0.8
16	39.5 35.2 38.6 34.2 37.0 37.2 36.8	7	36.9	1.7

Table 3-3. Velocity of Sound in Various Tissues, Air and Water

Tissue	Velocity of Sound (m/sec)	Density (g/cm^3)	Reference
Muscle	1580	1	Ludwig (1950), Frucht (1953), von Gierke (1964)
Fat	1450	1	Ludwig (1950), Fruch (1953)
Bone	3500	2.0	Clemedson & Jönsson (1961)
Ribs & intercostal muscle	<1000		Clemedson & Jönsson (1961)
Collapsed lung	650 (ultrasound)	0.4	Dunn & Fry (1961)
Collapsed lung pneumonitis	320 (ultrasound)	0.8	Dunn & Fry (1961)
Lung, air filled, horse	25	0.6	Rice (1983)
Lung, air filled, horse	70	0.125	Rice (1983)
Lung, air filled, calf	24-30		Clemedson & Jönsson (1962)
Air	340		Dunn & Fry (1961)
Water, distilled, 0°C	1407		Kaye & Laby (1960)
Air bubbles (45% by vol.) in glycerol & H_2O	20		Campbell & Pitcher (1958)

speed c^2 is proportional to the Young's modulus E and inversely proportional to tissue density ρ. Both E and ρ change with the transmural pressure, but when the lung is drained of blood the primary effect is a reduction of the density of the lung parenchyma; and a rise in wave speed is expected. Rice (1983) used He, air, and SF_6 in his experiments, and showed that the lower the density of the gas the higher the wave speed.

REFERENCES

Campbell, I. J. and A. S. Pitcher, "Shock Wave in a Liquid Containing Gas Bubbles," Proc. Roy. Soc. (London), Ser. A, 243, pp. 534-545 (1958).

Clemedson, C. J. and A. Jönsson, "Transmission and Reflection of High Explosive Shock Waves in Bone," Acta. Physiol. Scand. 51, pp. 47-61 (1961).

Clemedson, C. J. and A. Jönsson, "Distribution of Extra- and Intra-thoracic Pressure Variations in Rabbits Exposed to Air Shock Waves," Acta. Physiol. Scand., 54, pp. 18-29 (1962).

Corey, E. L., "Medical Aspects of Blast," Nav. Med. Bull. (Wash.), 46, pp. 623-652 (1946).

Dunn, F. and W. J. Fry, "Ultrasonic Absorption and Reflection by Lung Tissue," Physics Med. Biol., 5, pp. 401-410 (1961).

Frucht, A.-H., "Die Schallgeschwindigkeit in Menschlichen und Tierischen Geweben," Z. Ges. Exp. Med., 120, pp. 526-557 (1953).

Fung, Y. C., "Stress-Strain-History Relations of Soft Tissues in Simple Elongation," in Biomechanics (Fung, Editor), pp. 181-208, Prentice-Hall, New York, 1971.

Fung. Y. C., "Stress, Deformation, and Atalectasis of Ku Lung," Circulation Res., 37, pp. 481-496 (1975).

Fung, Y. C., Biomechanics: Mechanical Properties of Living Tissues, Springer-Verlag, New York, 1981.

Kaye, G. W. C. and T. H. Laby, Tables of Physical and Chemical Constants, 12th Ed., Longmans, Green, New York, 1960.

Ludwig, G. D., "The Velocity of Sound Through Tissues and the Acoustic Impedance of Tissues," J. Acoustic Soc. Amer., 22, pp. 862-866 (1950).

Rice, D. A., "Sound Speed in Pulmonary Parenchyma," J. Appl. Physiol.: Respir. Envir. Exercise Physiol., 54(1), pp. 304-308 (1983).

Schardin, H., "The Physical Principles of the Effects of a Detonation," Chapter XIV-A in German Aviation Medicine, World War II, Vol. 2, pp. 1207-1224, Depart. Air Force, U. S. Government Printing Office, Washington, DC, 1950.

Vawter, D. L., Y. C. Fung, and J. B. West, "Elasticity of Excised Dog Lung Parenchyma," J. Appl. Physiol., 45, pp. 261-269 (1978).

Vawter, D. L., Y. C. Fung, and J. B. West, "Constitutive Equation of Lung Tissue Elasticity," J. Biomech. Engrg., 101, pp. 38-45 (1979).

von Gierke, H. E., "Biodynamic Response of Human Body," Appl. Mech. Rev., 17, pp. 951-958 (1964).

White, C. S. and D. R. Richmond, "Blast Biology," Technical Progress Report TID-5764, Lovelace Foundation for Medical Education and Research, Albuquerque, New Mexico.

DISTRIBUTION LIST

12 copies	Director Walter Reed Army Institute of Research Walter Reed Army Medical Center ATTN: SGRD-UWZ-C Washington, DC 20307-5100
1 copy	Commander US Army Medical Research and Development Command ATTN: SGRD-RMI-S Fort Detrick, Frederick, MD 21701-5012
12 copies	Defense Technical Information Center (DTIC) ATTN: DTIC-DDAC Cameron Station Alexandria, VA 22304-6145
1 copy	Dean School of Medicine Uniformed Services University of the Health Sciences 4301 Jones Bridge Road Bethesda, MD 20814-4799
1 copy	Commandant Academy of Health Sciences, US Army ATTN: AHS-CDM Fort Sam Houston, TX 78234-6100